Variational solution to the lattice Boltzmann method for Couette flow

Joseph T. Johnson [1], Mahyar Madadi [2], Daniel R. Ladiges [3], Yong Shi [4], Barry D. Hughes [1], and John E. Sader [5,*]

[1] *School of Mathematics and Statistics, University of Melbourne, Victoria 3010, Australia*

[2] *Department of Materials Physics, Research School of Physics, Australian National University, Canberra, ACT 2601, Australia*

[3] *Center for Computational Sciences and Engineering, Lawrence Berkeley National Laboratory, Berkeley, California 94720, USA*

[4] *Department of Mechanical, Materials and Manufacturing Engineering, University of Nottingham Ningbo China, Ningbo 315100, China*

[5] *Graduate Aerospace Laboratories and Department of Applied Physics, California Institute of Technology, Pasadena, California 91125, USA*

(Received 4 October 2023; accepted 16 April 2024; published 29 May 2024)

Literature studies of the lattice Boltzmann method (LBM) demonstrate hydrodynamics beyond the continuum limit. This includes exact analytical solutions to the LBM, for the bulk velocity and shear stress of Couette flow under diffuse reflection at the walls through the solution of equivalent moment equations. We prove that the bulk velocity and shear stress of Couette flow with Maxwell-type boundary conditions at the walls, as specified by two-dimensional isothermal lattice Boltzmann models, are inherently linear in Mach number. Our finding enables a systematic variational approach to be formulated that exhibits superior computational efficiency than the previously reported moment method. Specifically, the number of partial differential equations (PDEs) in the variational method grows linearly with quadrature order while the number of moment method PDEs grows quadratically. The variational method directly yields a system of linear PDEs that provide exact analytical solutions to the LBM bulk velocity field and shear stress for Couette flow with Maxwell-type boundary conditions. It is anticipated that this variational approach will find utility in calculating analytical solutions for novel lattice Boltzmann quadrature schemes and other flows.

DOI: 10.1103/PhysRevE.109.055305

I. INTRODUCTION

Optimizing the operation of micro- and nanoscale devices under ambient conditions has inspired recent investigations in rarefied gas dynamics [1,2]. The theoretical framework used in many of these studies is based on the Boltzmann equation [3–5], which is an evolution equation for the (statistical) distribution function of molecular gas velocities. Frequently, the Bhatnagar-Gross-Krook (BGK) model [6] is used for the collision term in the Boltzmann equation, as we do here.

For steady flow, the regime of gas flow is embodied in the Knudsen number,

$$\mathrm{Kn} \equiv \frac{l}{L}, \tag{1}$$

which is the ratio of the mean free path of the gas, l, to the bulk length scale of the flow, L. The mean free path, l, is in turn related to the mean collision-free time of the gas, τ, by

$$l = c_s \tau, \tag{2}$$

where c_s is the speed of sound. The motion of macroscale devices generates continuum flows that are typically modeled by the Navier-Stokes equations, which are valid where the Knudsen number is small, i.e., $\mathrm{Kn} \ll 1$. However, micro- and nanoscale devices generate rarefied flows ($\mathrm{Kn} \not\to 0$), necessitating the use of alternate theories, such as the Boltzmann equation, that can accommodate arbitrary degrees of rarefaction. Another relevant parameter to these flows is the Mach number, Ma, which is the ratio of the device speed, U_0, to the speed of sound, c_s. The operation of small-scale devices perturbs the distribution function of the surrounding gases from thermodynamic equilibrium, generating slow flows for which [7]

$$\mathrm{Ma} \equiv \frac{U_0}{c_s} \ll 1,$$

that may be modeled by the Boltzmann equation linearized about this global equilibrium. Moment [8–10] and variational [11] methods are analytical techniques that may be used to study the Boltzmann equation, with the variational method requiring that the Boltzmann equation is linearized.

Grad's moment methods are derived either from (i) a Hermite-polynomial expansion of the distribution function in the vicinity of a local thermodynamic equilibrium, e.g., Grad's 13-moment theory [8] [[9], Section 28], or (ii) a global equilibrium with application to the (low Mach number) linearized Boltzmann equation [[9], Section 30]. The coefficients of both types of expansions are moments of the distribution function that represent the macroscopic quantities of the gas, such as its density and bulk velocity. Partial differential equations (PDEs) for these coefficients are derived by taking moments of the Boltzmann equation. Solving this system of PDEs provides an approximation of the distribution function and its moments. Alternately, numerical methods may be used to determine the distribution function and its moments to a desired level of accuracy. These numerical methods are

*jsader@caltech.edu

broadly characterized as either deterministic, such as the lattice Boltzmann method (LBM) [12,13], or stochastic, like the Monte Carlo method [14–16]. The standard LBM solves the Boltzmann equation on a grid of spatial nodes where the displacement between the nodes coincides with the elements of a velocity-space lattice. Further developments have shown that the spatial grids can be decoupled from these lattices [17,18]. These velocity-space lattices are selected based on achieving an accurate quadrature evaluation of the macroscopic variables that are moments of the distribution function.

At thermodynamic equilibrium, the distribution function for a monatomic ideal gas is a Gaussian function in particle velocity space. This suggests the use of Gauss-Hermite [19,20] or half-space Gauss-Hermite quadrature [18] to calculate the moments of the Gaussian function exactly up to $(2N-1)$th order, with at least N abscissas and weights. This property of Gauss-Hermite quadrature prompted Cercignani's remark, "If we choose the velocities $\boldsymbol{\xi}_i$ to be located at the zeroes of the Hermite polynomials $H_k(\boldsymbol{\xi})$, and a related interpolation formula is used, then the method of discrete ordinates is essentially equivalent to a moment method based on an expansion ...about a fixed rather than a local Maxwellian" [[3], p. 354]. The focus of the present work is the LBM. Thus, all subsequent expansions of the distribution function are performed about the (fixed) global equilibrium.

The equivalence between the LBM (a specific example of a discrete-ordinates method) and a moment method was derived explicitly by Shan and He [10]. Projecting a function onto the Hilbert space spanned by the N lowest-order one-dimensional Hermite polynomials requires calculating the moments of a Gaussian function up to order $2N$. This projection is performed exactly through Gauss-Hermite quadrature by utilizing $n = \lceil (2N+1)/2 \rceil = N+1$ abscissas and weights. Shan and He [10] extended this equivalence to the multidimensional case. For example, a distribution function depending on two velocity-space coordinates, $\boldsymbol{c} = (c_x, c_y)$, may be projected onto the space of tensor Hermite polynomials up to order $\boldsymbol{M} = (M_x, M_y)$, i.e., up to order M_x in c_x and order M_y in c_y, with at least (M_x+1, M_y+1) abscissas and weights. This thereby proves that an (M_x, M_y)-order moment method distribution function is equivalent to that provided by the LBM on a $D1Q(M_x+1) \times D1Q(M_y+1)$ velocity set; the latter uses (M_x+1, M_y+1)-order Gauss-Hermite quadrature. This equivalence provides a means of calculating analytical solutions to the LBM through the moment method. It also describes the error in the LBM as the truncation error in a Hermite-polynomial expansion of the distribution function. Shan and He commented as follows: "This error is negligible at small Mach numbers and can always be made smaller by using a quadrature of a higher degree" [[10], p. 68]. The present study develops this point, for two-dimensional isothermal discrete-velocity lattice Boltzmann models, in the case of steady Couette flow. Specifically, we show that the bulk velocity and shear stress are inherently linear in Mach number, deriving a novel equivalence between the nonlinear LBM and linearized solutions to steady Couette flow.

Ansumali *et al.* [21] applied diffuse boundary conditions to a moment method solution of the Boltzmann-BGK equation. In contrast to Grad's 13-moment theory that expands the distribution function about a local equilibrium, Ansumali *et al.* [21] expanded the distribution function about the global equilibrium. In doing so, they determined exact analytical solutions to the nonlinear isothermal lattice Boltzmann hierarchy. These exact solutions were demonstrated for steady Couette flow on (i) the $D2Q9 = D1Q3 \times D1Q3$ lattice (as is further elaborated on by Yudistiawan *et al.* [22]) and (ii) the $D2Q16$ lattice by solving systems of 9 and 16 coupled nonlinear PDEs, respectively [23]. The present study first reports the moment method approach of Ansumali *et al.* [21], using the Hermite-polynomial basis detailed by Grad [8,9] and Shan and He [10]. We invoke Maxwell-type boundary conditions for this solution, generalizing the diffuse boundary condition at the solid walls (reported in Ref. [21]) to incorporate specular boundary interactions with an accommodation coefficient.

Our work reveals that the bulk velocity and shear stress are part of a subset of moments of the distribution function, whose moment equations and boundary conditions linearly decouple from the other moments. This enables the calculation of these linearized quantities with only two quadrature points parallel to the bounding walls of the flow or, equivalently, a first-order expansion of the distribution function in the particle velocity parallel to the walls. Consequently, the bulk velocity and shear stress for the $D1Q(M_x+1) \times D1Q(M_y+1)$ lattice Boltzmann model can be determined exactly from M_y+1 linear PDEs—instead of $(M_x+1)(M_y+1)$ nonlinear PDEs derived through the moment method of Ansumali *et al.* [21]. Because the bulk velocity and shear stress moments are linear in Mach number, their governing equations—consisting of M_y+1 linear PDEs and associated boundary conditions—are shown to be most efficiently derived from a variational solution to the linearized Boltzmann-BGK equation. To illustrate this efficiency improvement, consider the (commonly used) symmetric $D1Q(M+1) \times D1Q(M+1) = D2Q(M+1)^2$ lattice Boltzmann model, e.g., $D2Q9$ or $D2Q16$. The number of linear PDEs for the bulk velocity and shear stress that arise from the variational method grows linearly with quadrature order, $M+1$. In contrast, evaluation of these same transport variables using the nonlinear moment equations grows quadratically with M, i.e., $(M+1)^2$. This can represent a dramatic improvement in efficiency.

The variational principle generally establishes an equivalence between the kernel of a self-adjoint linear operator and the stationary points of a functional. Despite the linearized Boltzmann-BGK operator not being self-adjoint, Cercignani [11,24] was able to formulate a variational principle for solutions to the linearized Boltzmann-BGK equation by shifting the standard functional using a carefully chosen boundary product. Cercignani demonstrated the utility of the variational method by calculating the velocity slip in Couette flow from two judiciously selected trial distributions [11]. Subsequently, the variational method has been used to calculate (i) plane Poiseuille flow subject to Maxwell-type boundary conditions with different accommodation coefficients [25], (ii) combined Couette-Poiseuille flow [26], and (iii) higher-order velocity slip coefficients [27,28]. In each case, the distribution function was represented by a carefully chosen trial solution based on known asymptotic results or properties of the flow. This method was generalized to unsteady oscillatory rarefied flows by Ladiges and Sader [29]—by expressing the distribution

function as a (normal) polynomial expansion of particle velocity space—to solve oscillatory Couette flow and Stokes's second problem. The parameters of this representation of the distribution function were then derived using the calculus of variations [11].

The present study uses a general Hermite-polynomial expansion of the distribution function about the global equilibrium to formulate a systematic variational approach for the LBM. It thereby enables direct access to the required moments of the flow. This variational approach also presents a substantial improvement in computational efficiency over the moment method described above. Specifically, it directly produces the required $M_y + 1$ linear PDEs and associated boundary conditions for steady Couette flow with Maxwell-type boundary conditions at the solid walls. This system of equations is solved to give exact analytical solutions for the LBM bulk velocity and shear stress together with other associated transport variables.

This study is organized as follows. Section II reports the steady Boltzmann-BGK equation and associated Maxwell-type boundary conditions. Section II A gives the corresponding system of equations for steady Couette flow that arise from the two-dimensional isothermal lattice Boltzmann model, which is the foundation of this study. In Sec. III, a moment method that makes use of a Hermite-polynomial expansion of the distribution function is formulated for Maxwell-type boundary conditions at the walls, generalizing the diffuse reflection formulation of Ref. [21] that used normal polynomials. The proposed variational approach is then reported in Sec. IV. Specifically, the linearized Boltzmann-BGK equation for steady Couette flow is presented in Sec. IV A, which forms the basis for the variational approach detailed in Sec. IV B. Section V applies the governing equations for the bulk velocity and shear stress—most efficiently generated by the variational approach (and identical to those of the moment method)—to derive exact analytical solutions to the $D2Q9$ lattice Boltzmann model for steady Couette flow under Maxwell-type boundary conditions. A summary of our findings is given in Sec. VI. Some mathematical details are relegated to Appendix A and the Supplemental Material [30], with the exact analytical solution to the $D2Q16$ lattice Boltzmann model for Couette flow given in Sec. S7 of the Supplemental Material [30]. A Mathematica notebook is also provided to facilitate implementation of the $D2Q9$ and $D2Q16$ exact analytical solutions for Couette flow.

II. BOLTZMANN-BGK EQUATION

The steady Boltzmann-BGK equation describes the evolution of the distribution function, $f(\boldsymbol{x}, \boldsymbol{c})$, for a gas in space, $\boldsymbol{x} \in \Omega \subset \mathbb{R}^3$, with particle velocity, $\boldsymbol{c} \in \mathbb{R}^3$,

$$\boldsymbol{c} \cdot \frac{\partial f}{\partial \boldsymbol{x}} = \frac{f^{\rm eq} - f}{\tau}, \tag{3}$$

where the mean collision-free time for each particle is τ [as given in Eq. (2)], and the local equilibrium distribution function is

$$f^{\rm eq} = \rho \left(\frac{m}{2\pi k_B T} \right)^{\frac{3}{2}} \exp\left(-\frac{m|\boldsymbol{c} - \boldsymbol{U}|^2}{2k_B T} \right). \tag{4}$$

Here m, ρ, $\boldsymbol{U}$, and T are the particle mass, gas density, bulk velocity, and temperature, respectively, while k_B is Boltzmann's constant. Requiring the BGK collision model [6] to conserve mass, momentum and energy,

$$\begin{bmatrix} 0 \\ \boldsymbol{0} \\ 0 \end{bmatrix} = \int_{\mathbb{R}^3} \begin{bmatrix} m \\ m\boldsymbol{c} \\ m|\boldsymbol{c}|^2 \end{bmatrix} (f^{\rm eq} - f)\, d\boldsymbol{c}, \tag{5}$$

and substituting Eq. (4) into Eq. (5), leads to definitions for the density, bulk velocity, and temperature as moments of the distribution function:

$$\begin{bmatrix} \rho \\ \rho \boldsymbol{U} \\ 3\rho k_B T/m \end{bmatrix} = \int_{\mathbb{R}^3} \begin{bmatrix} 1 \\ \boldsymbol{c} \\ |\boldsymbol{c} - \boldsymbol{U}|^2 \end{bmatrix} f d\boldsymbol{c}, \tag{6}$$

where these and all subsequent velocity space integrals are in Cartesian coordinates. The definition of $\rho \boldsymbol{U}$ in Eq. (6) shows that this quantity is the gas particle flux. The momentum flux (pressure tensor), $\boldsymbol{P}$, defined by

$$\boldsymbol{P} = \int_{\mathbb{R}^3} \boldsymbol{c}\,\boldsymbol{c} f\, d\boldsymbol{c},$$

can be partitioned into a macroscopic momentum flux, $\rho \boldsymbol{U}\boldsymbol{U}$, and a momentum flux due to thermal motion:

$$\begin{aligned} \boldsymbol{P} &= \int_{\mathbb{R}^3} ([\boldsymbol{c} - \boldsymbol{U}] + \boldsymbol{U})([\boldsymbol{c} - \boldsymbol{U}] + \boldsymbol{U}) f\, d\boldsymbol{c} \\ &= \rho \boldsymbol{U}\boldsymbol{U} + \int_{\mathbb{R}^3} (\boldsymbol{c} - \boldsymbol{U})(\boldsymbol{c} - \boldsymbol{U}) f\, d\boldsymbol{c}. \end{aligned}$$

That is, $\boldsymbol{P} = \rho \boldsymbol{U}\boldsymbol{U} + \mathfrak{P}$, where the thermal momentum flux (the stress tensor) is given by

$$\mathfrak{P} = \int_{\mathbb{R}^3} (\boldsymbol{c} - \boldsymbol{U})(\boldsymbol{c} - \boldsymbol{U}) f d\boldsymbol{c}. \tag{7}$$

The equation of state for this BGK gas is therefore

$$\mathrm{Tr}(\mathfrak{P}) = \frac{3\rho k_B T}{m}, \tag{8}$$

where Tr refers to the trace. The boundary of the spatial region, $\boldsymbol{x} \in \Omega$, occupied by the gas is denoted by $\partial\Omega$. We also denote by $\boldsymbol{n}$ the unit vector normal to this boundary, directed to the interior of Ω. The velocity of the boundary is denoted by $\boldsymbol{U}_{\partial\Omega}$. At each point, $\boldsymbol{x} \in \partial\Omega$, the boundary temperature, $T_{\partial\Omega}$, is taken to be prescribed. We impose Maxwell-type boundary conditions [31] on $\partial\Omega$, i.e., we allow a prescribed fraction of particles colliding with the boundary to be released diffusely, with the remainder reflected specularly, by use of the accommodation coefficient, $\alpha \in [0, 1]$. There is specular reflection only if $\alpha = 0$, while $\alpha = 1$ corresponds to purely diffuse release. For $\boldsymbol{x} \in \partial\Omega$ and $(\boldsymbol{c} - \boldsymbol{U}_{\partial\Omega}) \cdot \boldsymbol{n} > 0$, we have

$$\begin{aligned} f(\boldsymbol{x}, \boldsymbol{c}) = (1 - \alpha) f(\boldsymbol{x}, \boldsymbol{c} - 2\boldsymbol{n}(\boldsymbol{c} - \boldsymbol{U}_{\partial\Omega}) \cdot \boldsymbol{n}) \\ + \alpha \rho_{\partial\Omega}(\boldsymbol{x}) f^{\rm eq}_{\rm BC}(\boldsymbol{c}), \end{aligned} \tag{9}$$

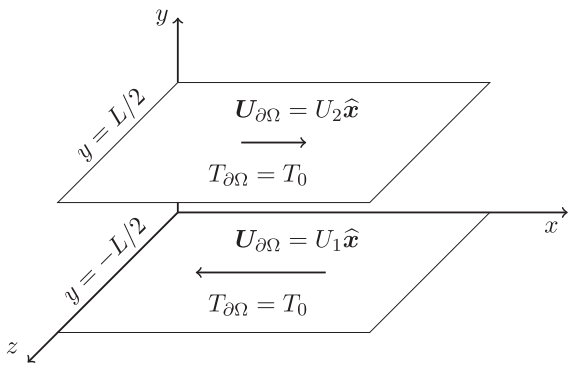

FIG. 1. Steady Couette flow between shearing parallel walls of infinite extent, held at the same temperature, T_0, and separated by a distance, L.

where

$$f^{\mathrm{eq}}_{\mathrm{BC}}(\boldsymbol{c}) = \left(\frac{m}{2\pi k_B T_{\partial\Omega}}\right)^{\frac{3}{2}} \exp\left(-\frac{m|\boldsymbol{c}-\boldsymbol{U}_{\partial\Omega}|^2}{2k_B T_{\partial\Omega}}\right), \tag{10}$$

and $\rho_{\partial\Omega}(\boldsymbol{x})$ is the boundary density, which can be expressed in terms of integrals over the half space, $(\boldsymbol{c}-\boldsymbol{U}_{\partial\Omega})\cdot\boldsymbol{n} < 0$. This is achieved by integrating the boundary condition in Eq. (9), over the region of velocity space in which it holds, using $\boldsymbol{c} - 2\boldsymbol{n}(\boldsymbol{c}-\boldsymbol{U}_{\partial\Omega})\cdot\boldsymbol{n}$ as the integration variable in the integral involving f on the right-hand side, and exploiting the conservation of mass condition,

$$\int_{\mathbb{R}^3} (\boldsymbol{c}-\boldsymbol{U}_{\partial\Omega})\cdot\boldsymbol{n} f(\boldsymbol{x},\boldsymbol{c}) d\boldsymbol{c} = 0 \quad \text{if} \quad \boldsymbol{x}\in\partial\Omega. \tag{11}$$

This leads to

$$\rho_{\partial\Omega}(\boldsymbol{x}) = \frac{\int_{(\boldsymbol{c}-\boldsymbol{U}_{\partial\Omega})\cdot\boldsymbol{n}<0} (\boldsymbol{c}-\boldsymbol{U}_{\partial\Omega})\cdot\boldsymbol{n} f\, d\boldsymbol{c}}{\int_{(\boldsymbol{c}-\boldsymbol{U}_{\partial\Omega})\cdot\boldsymbol{n}<0} (\boldsymbol{c}-\boldsymbol{U}_{\partial\Omega})\cdot\boldsymbol{n} f^{\mathrm{eq}}_{\mathrm{BC}}\, d\boldsymbol{c}}. \tag{12}$$

A. Steady Couette flow

This study focuses on Couette flow driven by steadily shearing parallel walls of separation, L; see Fig. 1. The velocities of the bottom and top walls are $U_1\widehat{\boldsymbol{x}}$ and $U_2\widehat{\boldsymbol{x}}$, respectively, so that the bulk velocity of the gas is

$$\boldsymbol{U}_{\partial\Omega}(y) = U_{\partial\Omega}(y)\widehat{\boldsymbol{x}}, \tag{13}$$

where

$$U_{\partial\Omega}(y) = \begin{cases} U_2, & y = \frac{L}{2}, \\ U_1, & y = -\frac{L}{2}. \end{cases}$$

The temperature boundary condition at the walls is

$$T_{\partial\Omega} = T_0.$$

The Boltzmann-BGK equation in Eq. (3) and its boundary conditions are translationally invariant with respect to the Cartesian coordinates, x and z. We enforce the condition that the bulk flow is spatially invariant in the x direction. Therefore, the time-invariant distribution function is independent of the spatial positions, x and z, and is denoted by $f(y, c_x, c_y, c_z)$; the subscripts, x, y, z, henceforth refer to the Cartesian components of the tensor quantity. The corresponding Maxwell-type boundary conditions are

$$f\left(\pm\frac{L}{2}, c_x, c_y \lessgtr 0, c_z\right) = (1-\alpha) f\left(\pm\frac{L}{2}, c_x, -c_y, c_z\right) + \alpha\rho_{\partial\Omega}\left(\pm\frac{L}{2}\right)\left(\frac{m}{2\pi k_B T_0}\right)^{\frac{3}{2}} \times \exp\left(-\frac{m}{2k_B T_0}\left\{\left[c_x - U_{\partial\Omega}\left(\pm\frac{L}{2}\right)\right]^2 + c_y^2 + c_z^2\right\}\right), \tag{14}$$

where for the upper wall, $y = L/2$, we require that $c_y < 0$; for the lower wall, $y = -L/2$, we require that $c_y > 0$. The gas densities on the walls, $y = \pm L/2$, are given by

$$\rho_{\partial\Omega}\left(\pm\frac{L}{2}\right) = \left(\frac{2\pi k_B T_0}{m}\right)^{\frac{3}{2}} \frac{\int_{\boldsymbol{c}\cdot\widehat{\boldsymbol{y}}\gtrless 0} c_y f\left(\pm\frac{L}{2}, c_x, c_y, c_z\right) d\boldsymbol{c}}{\int_{\boldsymbol{c}\cdot\widehat{\boldsymbol{y}}\gtrless 0} c_y \exp\left(-\frac{m}{2k_B T_0}\left\{\left[c_x - U_{\partial\Omega}\left(\pm\frac{L}{2}\right)\right]^2 + c_y^2 + c_z^2\right\}\right) d\boldsymbol{c}}. \tag{15}$$

In Eqs. (14) and (15), and also below for brevity, we provide boundary conditions for both walls as a single equation. In the domains of integration, the upper inequality is taken when $y = L/2$, whereas the lower inequality is for $y = -L/2$. The variables and parameters of this system are scaled using the mean collision-free time, τ, speed of sound,

$$c_s = \sqrt{\frac{k_B T_0}{m}},$$

and the equilibrium gas density, ρ_0, i.e., in the absence of the walls, and the Knudsen number, Kn. We therefore define the following (dashed) dimensionless variables:

$$f = \rho_0 c_s^{-3} f', \quad f^{\mathrm{eq}} = \rho_0 c_s^{-3} f^{\mathrm{eq}\prime}, \quad \rho = \rho_0\rho',$$
$$\boldsymbol{U} = c_s\boldsymbol{u}, \quad \boldsymbol{U}_{\partial\Omega} = c_s\boldsymbol{u}_{\partial\Omega},$$
$$T = T_0 T', \quad \boldsymbol{x} = L\boldsymbol{x}', \quad \boldsymbol{P} = \rho_0 c_s^2 \boldsymbol{P}', \quad \boldsymbol{\mathfrak{P}} = \rho_0 c_s^2 \boldsymbol{\mathfrak{P}}',$$
$$\rho_{\partial\Omega} = \rho_0 \rho'_{\partial\Omega}, \quad \boldsymbol{c} = c_s\boldsymbol{c}'$$
$$U_2 = c_s u_2, \quad U_1 = c_s u_1.$$

Substituting the dimensionless quantities into the steady Boltzmann-BGK equation, Eq. (3), and omitting the " ′ "

notation for brevity, gives the dimensionless Boltzmann-BGK equation,

$$\boldsymbol{c}\cdot\frac{\partial f}{\partial \boldsymbol{x}}=\frac{1}{\mathrm{Kn}}(f^{\mathrm{eq}}-f), \tag{16}$$

where the dimensionless local equilibrium is

$$f^{\mathrm{eq}}(\boldsymbol{c})=\frac{\rho}{(2\pi)^{\frac{3}{2}}}\exp\left(-\frac{|\boldsymbol{c}-\boldsymbol{u}|^2}{2T}\right), \tag{17}$$

and the dimensionless moments of the distribution function are

$$\begin{bmatrix}\rho\\ \rho\boldsymbol{u}\\ 3\rho T\\ \boldsymbol{P}\\ \mathfrak{P}\end{bmatrix}=\int_{\mathbb{R}^3}\begin{bmatrix}1\\ \boldsymbol{c}\\ |\boldsymbol{c}-\boldsymbol{u}|^2\\ \boldsymbol{c}\,\boldsymbol{c}\\ (\boldsymbol{c}-\boldsymbol{u})(\boldsymbol{c}-\boldsymbol{u})\end{bmatrix}f d\boldsymbol{c}.$$

The dimensionless Maxwell-type boundary conditions on the walls, $y=\pm 1/2$ (for $c_y\lessgtr 0$ when $y=\pm 1/2$), are

$$\begin{aligned}f\left(\pm\frac{1}{2},c_x,c_y,c_z\right)&=(1-\alpha)f\left(\pm\frac{1}{2},c_x,-c_y,c_z\right)\\&\quad+\alpha\frac{\rho_{\partial\Omega}\left(\pm\frac{1}{2}\right)}{(2\pi)^{\frac{3}{2}}}\\&\quad\times\exp\left(-\frac{\left[c_x-u_{\partial\Omega}\left(\pm\frac{1}{2}\right)\right]^2+c_y^2+c_z^2}{2}\right),\end{aligned} \tag{18}$$

where

$$\rho_{\partial\Omega}\left(\pm\frac{1}{2}\right)=\frac{(2\pi)^{\frac{3}{2}}\int_{\boldsymbol{c}\cdot\hat{\boldsymbol{y}}\lessgtr 0}c_y f\left(\pm\frac{1}{2},c_x,c_y,c_z\right)d\boldsymbol{c}}{\int_{\boldsymbol{c}\cdot\hat{\boldsymbol{y}}\lessgtr 0}c_y\exp\left(-\frac{[c_x-u_{\partial\Omega}(\pm\frac{1}{2})]^2+c_y^2+c_z^2}{2}\right)d\boldsymbol{c}}. \tag{19}$$

The integral in the denominator of Eq. (19) could be evaluated exactly at this point. However, LBM evaluates the integrals in Eq. (19) using quadrature [21]. To replicate the LBM solution via the moment method in Sec. III, we refrain from evaluating the integral in the denominator here. We exhibit the relevant quadrature approximation of Eq. (19) in Eq. (S1.18) of the Supplemental Material [30] and use the exact evaluation of its denominator in Sec. IV A.

We consider the lattice Boltzmann model particle velocities to be confined to the xy plane and enforce isothermal flow in this lattice Boltzmann model, i.e., $T=1$ [21]. This enables f to be expressed as the (isothermal) reduced distribution function,

$$\widetilde{f}(y,c_x,c_y)\equiv\sqrt{2\pi}\exp\left(\frac{c_z^2}{2}\right)f(y,c_x,c_y,c_z), \tag{20}$$

whose Boltzmann-BGK equation follows directly from Eq. (16),

$$c_y\frac{\partial\widetilde{f}}{\partial y}=\frac{1}{\mathrm{Kn}}(\widetilde{f}^{\mathrm{eq}}-\widetilde{f}). \tag{21}$$

Here the local equilibrium is

$$\widetilde{f}^{\mathrm{eq}}=\frac{\rho}{2\pi}\exp\left(-\frac{(c_x-u)^2+(c_y-v)^2}{2}\right), \tag{22}$$

and

$$\begin{bmatrix}\rho\\ \rho u\\ \rho v\\ P_{xx}\\ P_{xy}\\ \mathfrak{P}_{xy}\\ P_{yy}\end{bmatrix}=\int_{-\infty}^{\infty}\int_{-\infty}^{\infty}\begin{bmatrix}1\\ c_x\\ c_y\\ c_x^2\\ c_xc_y\\ (c_x-u)(c_y-v)\\ c_y^2\end{bmatrix}\widetilde{f}dc_xdc_y. \tag{23}$$

The dimensionless energy flux, $\boldsymbol{Q}$, in the resulting two-dimensional system is

$$\begin{bmatrix}Q_x\\ Q_y\end{bmatrix}=\int_{-\infty}^{\infty}\int_{-\infty}^{\infty}(c_x^2+c_y^2)\begin{bmatrix}c_x\\ c_y\end{bmatrix}\widetilde{f}dc_xdc_y. \tag{24}$$

The reduced distribution function, $\widetilde{f}$, is subject to the boundary conditions,

$$\begin{aligned}\widetilde{f}\left(\pm\tfrac{1}{2},c_x,c_y\right)&=(1-\alpha)\widetilde{f}\left(\pm\tfrac{1}{2},c_x,-c_y\right)\\&\quad+\alpha\rho_{\partial\Omega}\left(\pm\tfrac{1}{2}\right)\widetilde{f}^{\mathrm{eq}}_{\mathrm{BC}}\left(\pm\tfrac{1}{2},c_x,c_y\right),\end{aligned} \tag{25}$$

for $c_y\lessgtr 0$ when $y=\pm 1/2$, and

$$\widetilde{f}^{\mathrm{eq}}_{\mathrm{BC}}\left(\pm\frac{1}{2},c_x,c_y\right)=\frac{1}{2\pi}\exp\left(-\frac{\left[c_x-u_{\partial\Omega}\left(\pm\frac{1}{2}\right)\right]^2+c_y^2}{2}\right), \tag{26a}$$

$$\rho_{\partial\Omega}\left(\pm\frac{1}{2}\right)=\frac{\int_{\boldsymbol{c}\cdot\hat{\boldsymbol{y}}\lessgtr 0}c_y\widetilde{f}\left(\pm\frac{1}{2},c_x,c_y\right)dc_xdc_y}{\int_{\boldsymbol{c}\cdot\hat{\boldsymbol{y}}\lessgtr 0}c_y\widetilde{f}^{\mathrm{eq}}_{\mathrm{BC}}\left(\pm\frac{1}{2},c_x,c_y\right)dc_xdc_y}. \tag{26b}$$

III. THE MOMENT METHOD SOLUTION

The moment method approach of Ansumali *et al.* [21] is now used to derive PDEs and BCs for Couette flow under Maxwell-type boundary conditions with arbitrary gas accomodation at the solid walls [32]. These PDEs and BCs extend the results of Ref. [21], that only considered pure diffuse reflection at the walls, and will be used to benchmark the proposed variational solution. We note that the moment method of Ansumali *et al.* [21] involves an expansion of the distribution function in normal polynomials about the global equilibrium. This differs from Grad's 13-moment theory [8] [[9], Section 28] which employs a Hermite-polynomial expansion about a local equilibrium; see above.

The (isothermal) reduced distribution function, $\widetilde{f}$, in Eq. (20) is approximated by projecting it onto a subspace of velocity space spanned by Hermite polynomials, $\mathcal{H}_{m_x,m_y}$ [33], of dimension, $\boldsymbol{M}=(M_x,M_y)$,

$$\widetilde{f}\approx w_{2\mathrm{D}}\sum_{m_x=0}^{M_x}\sum_{m_y=0}^{M_y}a_{m_x,m_y}\mathcal{H}_{m_x,m_y}, \tag{27}$$

where the global equilibrium is

$$w_{2\mathrm{D}}(c_x,c_y)=\frac{1}{2\pi}\exp\left(-\frac{c_x^2+c_y^2}{2}\right).$$

The Hermite polynomials used here are defined in Sec. S1 of the Supplemental Material [30]. The position-dependent

coefficients, $a_{m_x,m_y}(y)$, are given by

$$a_{m_x,m_y} = m_x!\, m_y! \int_{-\infty}^{\infty}\int_{-\infty}^{\infty} \widetilde{f}\, \mathcal{H}_{m_x,m_y} dc_x dc_y, \tag{28}$$

which are moments of the velocity distribution function, including the mass flux (bulk velocity field) parallel to the walls, $a_{1,0} = \rho u$, and the shear stress distribution, $a_{1,1} = P_{xy}$. Multiplying both sides of the Boltzmann-BGK equation in Eq. (21) by $\mathcal{H}_{m_x,m_y}$, using the Hermite-polynomial recursion relation, and integrating over c_x and c_y, produces the PDEs:

$$\frac{\partial a_{m_x,1}}{\partial y} = \frac{1}{\mathrm{Kn}}\left(\frac{a_{1,0}^{m_x}}{a_{0,0}^{m_x-1}} - a_{m_x,0}\right), \tag{29a}$$

$$m_y \frac{\partial a_{m_x,m_y-1}}{\partial y} + \frac{\partial a_{m_x,m_y+1}}{\partial y} = \frac{1}{\mathrm{Kn}}\left(\frac{a_{1,0}^{m_x} a_{0,1}^{m_y}}{a_{0,0}^{m_x+m_y-1}} - a_{m_x,m_y}\right), \tag{29b}$$

$$M_y \frac{\partial a_{m_x,M_y-1}}{\partial y} = \frac{1}{\mathrm{Kn}}\left(\frac{a_{1,0}^{m_x} a_{0,1}^{M_y}}{a_{0,0}^{m_x+M_y-1}} - a_{m_x,M_y}\right), \tag{29c}$$

where $m_x = 0, 1, \ldots, M_x$ and $m_y = 1, \ldots, M_y - 1$, on application of the orthogonality relation between Hermite polynomials. We note that the system of moment equations in Eq. (29) is closed due to the use of a truncated expansion in Hermite polynomials [34]; see Eq. (27). This is equivalent to the use of a discrete-velocity set as highlighted by Shan and He [10].

These equations represent a coupled system of $(M_x + 1)(M_y + 1)$ nonlinear PDEs that needs to be solved, to evaluate the macroscopic quantities and the reduced distribution function for steady Couette flow. Note that Eq. (29a) is independent of m_y, a property which is used to determine the total number of coupled PDEs.

The system of PDEs in Eq. (29) may be simplified—as performed by Ansumali *et al.* [21] for diffuse reflection only—but the process is protracted. It is clear from Eq. (29) that all moments, a_{m_x,m_y}, with the same value of m_x are coupled, $(m_x,)$–moments. It follows that each such set of moments is coupled to (i) the (1,)–moments, through $a_{1,0}$, and (ii) the (0,)–moments, through $a_{0,0}$ and $a_{0,1}$, that appear in the right-hand side of Eq. (29). The (0,)–moments are solved with considerable effort and are reported in Secs. S1, S4, and S5 of the Supplemental Material [30]. This leaves the (1,)–moments to be evaluated to determine the remaining moments and the reduced distribution function. The (1,)–moments define the primary transport variables for steady Couette flow in the continuum limit, including the bulk velocity and shear stress. Its associated velocity slip coefficient is calculated from the bulk velocity field parallel to the walls [11,27–29].

Fortunately, the PDEs and boundary conditions that determine the (1,)–moments, a_{1,m_y}, are linear and decouple from the other moments; see Sec. S1 of the Supplemental Material [30]. This allows the (1,)–moments to be more efficiently calculated from a smaller system of linear equations than the moment PDEs in Eq. (29). Deducing this smaller set of linear PDEs and boundary conditions from Eq. (29)—by solving the (0,)–moments—is elaborate (see Secs. S1, S4, and S5 of the Supplemental Material [30]) and gives

$$\frac{\partial a_{1,1}}{\partial y} = 0, \tag{30a}$$

$$m_y \frac{\partial a_{1,m_y-1}}{\partial y} + \frac{\partial a_{1,m_y+1}}{\partial y} = -\frac{a_{1,m_y}}{\mathrm{Kn}}, \tag{30b}$$

$$M_y \frac{\partial a_{1,M_y-1}}{\partial y} = -\frac{a_{1,M_y}}{\mathrm{Kn}}, \tag{30c}$$

where $m_y = 1, \ldots, M_y - 1$, i.e., $M_y + 1$ coupled linear PDEs.

A reduced distribution function that is correct up to order (M_x, M_y) in (c_x, c_y), as shown in Eq. (27), is equivalent to a Gauss-Hermite quadrature approximation of the reduced distribution function on a lattice of $(M_x + 1, M_y + 1)$ abscissas, $\boldsymbol{c_i}$, and weights, ω_i, [10]

$$\boldsymbol{c_i} = \boldsymbol{c}_{i_x,i_y} = (c_{x,i_x}, c_{y,i_y}),$$
$$\omega_{\boldsymbol{i}} = \omega_{i_x,i_y} = w_{i_x} w_{i_y},$$

where $i_x \in [0, M_x]$ and $i_y \in [0, M_y]$. On this lattice, the boundary conditions for the (1,)–moments are

$$\sum_{m_y=0}^{M_y} \frac{a_{1,m_y}\left(\pm\frac{1}{2}\right)}{m_y!} H_{m_y}(c_{y,i_y}) = \alpha u_{\partial\Omega}\left(\pm\frac{1}{2}\right) + (1-\alpha)\sum_{m_y=0}^{M_y} \frac{(-1)^{m_y} a_{1,m_y}\left(\pm\frac{1}{2}\right)}{m_y!} H_{m_y}(c_{y,i_y}), \tag{31}$$

for $c_{y,i_y} \lessgtr 0$.

The PDEs in Eq. (30) and boundary conditions in Eq. (31) only depend on the (1,)–moments. They are also linear in the boundary velocities, $u_{\partial\Omega}(\pm\frac{1}{2}) = u_{2,1}$, and the (1,)–moments themselves. This suggests that the (1,)–moments may be identically derived from the linearized Boltzmann-BGK equation, which we prove in Sec. IV A. Only after the (1,)–moments have been calculated can the remaining moments and reduced distribution function in Eq. (27) be determined from Eq. (29).

In summary, use of the moment method requires the solution to the $(M_x + 1)(M_y + 1)$ coupled nonlinear PDEs defined in Eq. (29). After considerable effort, a simplified set of $M_y + 1$ coupled linear PDEs is generated in Eq. (30), with associated boundary conditions in Eq. (31). The next section details a more efficient means of arriving at this simplified set of linear PDEs and its associated boundary conditions, by using a variational approach for the linearized Boltzmann-BGK equation. This variational approach thus presents a substantial improvement in computational efficiency, by eliminating the need to solve the initial $(M_x + 1)(M_y + 1)$ coupled nonlinear PDEs.

IV. A VARIATIONAL SOLUTION FOR LOW-MACH-NUMBER COUETTE FLOW

We first review the linearized Boltzmann-BGK equation subject to Maxwell-type boundary conditions [[5], Section 1.11], which forms the basis for the proposed variational approach.

A. Linearized Boltzmann-BGK equation for low-Mach-number Couette flow

For two parallel walls moving with dimensionless velocities, u_1 and u_2, in their planes at low Mach number, i.e.,

$$|u_1|, |u_2| \ll 1,$$

the distribution function, f, of the gas is perturbed slightly from global thermodynamic equilibrium, giving

$$f(y, \boldsymbol{c}) = w_{3D}(\boldsymbol{c})[1 + \Phi(y, \boldsymbol{c}) + o(\Phi)], \tag{32}$$

with

$$w_{3D}(\boldsymbol{c}) = \frac{1}{(2\pi)^{\frac{3}{2}}} \exp\left(-\frac{c_x^2 + c_y^2 + c_z^2}{2}\right),$$

where $|\Phi| \ll 1$ is of order the Mach number. The macroscopic quantities may also be expanded about their values at thermodynamic equilibrium:

$$\begin{bmatrix} \rho \\ \boldsymbol{u} \\ T \\ \boldsymbol{P} \end{bmatrix} = \begin{bmatrix} 1 \\ \boldsymbol{0} \\ 1 \\ \boldsymbol{I} \end{bmatrix} + \begin{bmatrix} \eta \\ \boldsymbol{u} \\ \kappa \\ \boldsymbol{p} \end{bmatrix} + o(\Phi),$$

where $\boldsymbol{I}$ is the identity tensor, and

$$\begin{bmatrix} \eta \\ \boldsymbol{u} \\ \kappa \\ \boldsymbol{p} \end{bmatrix} = \int_{\mathbb{R}^3} \begin{bmatrix} 1 \\ \boldsymbol{c} \\ \frac{1}{3}|\boldsymbol{c}|^2 - 1 \\ \boldsymbol{c}\,\boldsymbol{c} \end{bmatrix} w_{3D}(\boldsymbol{c})\Phi(y, \boldsymbol{c})\, d\boldsymbol{c}. \tag{33}$$

Similarly, expanding the Boltzmann-BGK equation in Eq. (3) to linear order in Mach number gives

$$\mathrm{Kn}\, c_y \frac{\partial \Phi}{\partial y} = \eta + \boldsymbol{c} \cdot \boldsymbol{u} + \frac{\kappa}{2}(|\boldsymbol{c}|^2 - 3) - \Phi, \tag{34}$$

where we have retained the temperature dependence because there is no isothermal constraint imposed in this Sec. IV A. As we show below, the bulk velocity and stress are independent of temperature to linear order in Mach number. The same expansion of the boundary condition, Eq. (18), provides the required boundary condition on Φ:

$$\begin{aligned} \Phi\left(\pm\frac{1}{2}, c_x, c_y, c_z\right) = (1-\alpha)\Phi\left(\pm\frac{1}{2}, c_x, -c_y, c_z\right) \\ + \alpha c_x u_{\partial\Omega}\left(\pm\frac{1}{2}\right) \\ \pm \alpha\sqrt{2\pi} \int_{c_y \gtrless 0} c_y \Phi\left(\pm\frac{1}{2}, c_x, c_y, c_z\right) \\ \times\, w_{3D}(\boldsymbol{c}) d\boldsymbol{c}, \end{aligned} \tag{35}$$

for $c_y \lessgtr 0$. Equations (34) and (35) may be simplified to evaluate the (1,)–moments, such as the bulk velocity parallel to the walls and the shear stress, by considering the moment,

$$\widetilde{\Phi}(y, c_y) \equiv \int_{-\infty}^{\infty}\int_{-\infty}^{\infty} \widetilde{w}_{2D}(c_x, c_z) c_x \Phi(y, \boldsymbol{c}) dc_x dc_z,$$

where

$$\widetilde{w}_{2D}(c_x, c_z) = \frac{1}{2\pi} \exp\left(-\frac{c_x^2 + c_z^2}{2}\right).$$

Taking this moment of Eq. (34) and using the orthogonality of Hermite polynomials gives

$$\mathrm{Kn}\, c_y \frac{\partial}{\partial y}\widetilde{\Phi} = u - \widetilde{\Phi}, \tag{36}$$

where

$$\begin{bmatrix} u \\ p_{xy} \end{bmatrix} = \int_{-\infty}^{\infty} \begin{bmatrix} 1 \\ c_y \end{bmatrix} \widetilde{\Phi}(y, c_y)\, w_{1D}(c_y) dc_y,$$

and

$$w_{1D}(c_y) = \frac{1}{\sqrt{2\pi}} \exp\left(-\frac{c_y^2}{2}\right),$$

with the corresponding boundary conditions obtained by evaluating this same moment of Eq. (35),

$$\widetilde{\Phi}\left(\pm\tfrac{1}{2}, c_y\right) = \alpha u_{\partial\Omega}\left(\pm\tfrac{1}{2}\right) + (1-\alpha)\widetilde{\Phi}\left(\pm\tfrac{1}{2}, -c_y\right), \tag{37}$$

for $c_y \lessgtr 0$.

Equations (32), (36), and (37) show that there is no coupling of the bulk velocity and stress to the temperature perturbation, κ, at linear order in Mach number; the shear stress transfers heat into the gas at higher order in Mach number. Thus, the isothermal nonlinear bulk velocity and shear stress obtained by the moment method in Sec. III (which is equivalent to the nonlinear isothermal lattice Boltzmann model employing a two-dimensional discrete-velocity set) are identical to those that would obtained from the linearized Boltzmann equation. This establishes that the bulk velocity and shear stress for the nonlinear LBM are exactly recoverable from the linearized Boltzmann equation.

The next section will show that a variational approach to solving Eqs. (36) and (37) directly reproduces Eqs. (30) and (31) for the (1,)–moments and thus exhibits superior efficiency to the moment method.

B. Variational solution to the linearized Boltzmann-BGK equation

Cercignani [11] describes a variational approach to solving the linearized Boltzmann-BGK equation, for an arbitrary distribution function that is subject to kinetic boundary conditions. This includes the Maxwell-type boundary conditions used in this study.

We apply Cercignani's variational approach to steady Couette flow for a Hermite-polynomial expansion of the distribution function, subject to a quadrature approximation of Maxwell-type boundary conditions. The (1,)–moment PDEs in Eq. (30) and its boundary conditions in Eq. (31) are derived directly from this variational formulation using the Euler-Lagrange equations and natural boundary conditions, respectively. This eliminates the need for detailed analysis of the moment equations in Eq. (29), as was performed in the Sec. III. As we shall show, this approach provides a dramatic improvement in computational efficiency over the moment method, while recovering precisely the same results.

Cercignani's variational principle—Theorem 2 in Sec. S6 of the Supplemental Material [30]—establishes that solutions to the linearized Boltzmann-BGK equation, Eq. (36), satisfy the inhomogeneous boundary conditions in Eq. (37) if and

only if they are stationary points of the functional,

$$J[\widetilde{\Phi}] = \langle \widetilde{\Phi}, \mathbb{L}\widetilde{\Phi}\rangle_V + J_{\mathrm{HS}}[\widetilde{\Phi}]. \tag{38}$$

Here the linearized Boltzmann-BGK operator for steady Couette flow is defined by

$$\mathbb{L}\widetilde{\Phi} \equiv c_y \frac{\partial \widetilde{\Phi}}{\partial y} - \frac{1}{\mathrm{Kn}}\left\{\int_{-\infty}^{\infty}\left[w_{1\mathrm{D}}(c_y)\,\widetilde{\Phi}\right]dc_y - \widetilde{\Phi}\right\}, \tag{39}$$

which acts on the vector space of differentiable and integrable functions, V, accompanied by the inner product defined by Cercignani [[11], pp. 299–300] as

$$\langle g_1, g_2\rangle_V = \int_{-\frac{1}{2}}^{\frac{1}{2}}\int_{-\infty}^{\infty} w_{1\mathrm{D}}(c_y) g_1(y, c_y) g_2(y, -c_y)\, dc_y\, dy, \tag{40}$$

and the boundary product is

$$J_{\mathrm{HS}}[\widetilde{\Phi}] = \langle \widetilde{\Phi}, \widetilde{\Phi} - (1-\alpha)\widetilde{\Phi}(y, -c_y) - \alpha u_{\partial\Omega}(y)\rangle_B.$$

The (1,)–moments are sought by expressing the distribution function, $\widetilde{\Phi}$, as a full-space Hermite-polynomial expansion,

$$\widetilde{\Phi}(y, c_y) = \sum_{m_y=0}^{M_y} \frac{a_{1,m_y}(y)}{m_y!} H_{m_y}(c_y). \tag{41}$$

A full-space solution cannot produce the velocity space discontinuity induced by the diffuse component of the Maxwell-type conditions in Eq. (37). This issue is overcome by applying full-space Gauss-Hermite quadrature to these boundary conditions, so that Eq. (37) holds at Gauss-Hermite abscissa leaving the walls,

$$\begin{aligned}\widetilde{\Phi}(\mp 1/2, c_{y,i_y} \gtrless 0) = {} & (1-\alpha)\widetilde{\Phi}(\mp 1/2, -c_{y,i_y}) \\ & + \alpha u_{\partial\Omega}(\mp 1/2),\end{aligned} \tag{42}$$

for $c_{y,i_y} \gtrless 0$. For a full-space solution to satisfy these boundary conditions, this same quadrature must be applied to the boundary product,

$$\begin{aligned}J_{\mathrm{FS}}[\widetilde{\Phi}] = \Bigg\{ & \sum_{\mathrm{sgn}(y)c_{y,i_y}>0} c_{y,i_y} w_{i_y} \widetilde{\Phi}(y, c_{y,i_y}) \\ & \times [\widetilde{\Phi}(y, -c_{y,i_y}) - (1-\alpha)\widetilde{\Phi}(y, c_{y,i_y}) \\ & - 2\alpha u_{\partial\Omega}(y)]\Bigg\}_{y=-\frac{1}{2}}^{y=\frac{1}{2}},\end{aligned} \tag{43}$$

where

$$J[\widetilde{\Phi}] = \langle \widetilde{\Phi}, \mathbb{L}\widetilde{\Phi}\rangle_V + J_{\mathrm{FS}}[\widetilde{\Phi}], \tag{44}$$

and the $\mathrm{sgn}(y)$ function is defined by

$$\mathrm{sgn}(y) = \begin{cases} 1 & y > 0, \\ 0 & y = 0, \\ -1 & y < 0. \end{cases}$$

Quadrature need not be applied explicitly to the full-space integrals in the functional, $\langle \widetilde{\Phi}, \mathbb{L}\widetilde{\Phi}\rangle_V$, because they comprise full-space Gaussian moments that will be calculated exactly through quadrature.

Substituting the Hermite-polynomial expansion of the distribution function in Eq. (41) into the functional in Eq. (44), gives

$$J[\widetilde{\Phi}] = \int_{-\frac{1}{2}}^{\frac{1}{2}} \mathcal{L}\left(a_{1,m_y}, \frac{\partial a_{1,m_y}}{\partial y}\right) dy + J_{\mathrm{FS}}[\widetilde{\Phi}],$$

where

$$\mathcal{L} = \int_{-\infty}^{\infty} w_{1\mathrm{D}}(c_y)\widetilde{\Phi}(y, c_y)\mathbb{L}\widetilde{\Phi}(y, -c_y) dc_y. \tag{45}$$

Defining a deviation of the moments,

$$\widehat{a}_{1,m_y} = a_{1,m_y} + \epsilon\phi_{1,m_y},$$

allows the first variation of J to be written as

$$\delta J[\widetilde{\Phi}] = \lim_{\epsilon\to 0^+}\int_{-\frac{1}{2}}^{\frac{1}{2}} \frac{d}{d\epsilon}\mathcal{L}\left(\widehat{a}_{1,m_y}, \frac{\partial \widehat{a}_{1,m_y}}{\partial y}\right) dy + \delta J_{\mathrm{FS}}[\widetilde{\Phi}],$$

where

$$\delta J_{\mathrm{FS}}[\widetilde{\Phi}] = \lim_{\epsilon\to 0^+}\frac{d}{d\epsilon} J_{\mathrm{FS}}[\widehat{\widetilde{\Phi}}],$$

and

$$\widehat{\widetilde{\Phi}}(y, c_y) = \sum_{m_y=0}^{M_y} \frac{\widehat{a}_{1,m_y}(y)}{m_y!} H_{m_y}(c_y).$$

Application of the chain rule then gives

$$\begin{aligned}\delta J[\widetilde{\Phi}] = {} & \lim_{\epsilon\to 0^+}\sum_{m_y=0}^{M_y}\int_{-\frac{1}{2}}^{\frac{1}{2}}\Bigg[\frac{d\widehat{a}_{1,m_y}}{d\epsilon}\frac{\partial\mathcal{L}}{\partial\widehat{a}_{1,m_y}} + \frac{d}{d\epsilon}\left(\frac{\partial\widehat{a}_{1,m_y}}{\partial y}\right) \\ & \times \frac{\partial\mathcal{L}}{\partial\left(\frac{\partial}{\partial y}\widehat{a}_{1,m_y}\right)}\Bigg] dy + \delta J_{\mathrm{FS}}[\widetilde{\Phi}] \\ = {} & \lim_{\epsilon\to 0^+}\sum_{m_y=0}^{M_y}\int_{-\frac{1}{2}}^{\frac{1}{2}}\Bigg[\phi_{1,m_y}\frac{\partial\mathcal{L}}{\partial\widehat{a}_{1,m_y}} + \frac{\partial\phi_{1,m_y}}{\partial y} \\ & \times \frac{\partial\mathcal{L}}{\partial\left(\frac{\partial}{\partial y}\widehat{a}_{1,m_y}\right)}\Bigg] dy + \delta J_{\mathrm{FS}}[\widetilde{\Phi}].\end{aligned}$$

Integrating by parts and then taking the limit inside the integral gives

$$\begin{aligned}\delta J[\widetilde{\Phi}] = {} & \sum_{m_y=0}^{M_y}\int_{-\frac{1}{2}}^{\frac{1}{2}}\phi_{1,m_y}\left[\frac{\partial\mathcal{L}}{\partial a_{1,m_y}} - \frac{\partial}{\partial y}\frac{\partial\mathcal{L}}{\partial\left(\frac{\partial}{\partial y}a_{1,m_y}\right)}\right] dy \\ & + \delta J_{\mathrm{FS}}[\widetilde{\Phi}] \\ & + \sum_{m_y=0}^{M_y}\left[\phi_{1,m_y}\frac{\partial\mathcal{L}}{\partial\left(\frac{\partial}{\partial y}a_{1,m_y}\right)}\right]_{y=-\frac{1}{2}}^{y=\frac{1}{2}}.\end{aligned}$$

Because the perturbing functions, ϕ_{1,m_y}, are arbitrary, a variational solution (stationary points of the functional J) must zero each term in the first variation, i.e., they satisfy the Euler-Lagrange equations,

$$\frac{\partial\mathcal{L}}{\partial a_{1,m_y}} - \frac{\partial}{\partial y}\frac{\partial\mathcal{L}}{\partial\left(\frac{\partial}{\partial y}a_{1,m_y}\right)} = 0, \tag{46}$$

where $m_y = 0, 1, \ldots, M_y$, and zero the boundary terms, i.e.,

$$\sum_{m_y=0}^{M_y} \left[\phi_{1,m_y} \frac{\partial \mathcal{L}}{\partial\left(\frac{\partial}{\partial y} a_{1,m_y}\right)} \right]_{y=-\frac{1}{2}}^{y=\frac{1}{2}} + \delta J_{\mathrm{FS}}[\widetilde{\Phi}] = 0. \tag{47}$$

Next, we separately study the boundary terms in Eq. (47) and the governing equation in Eq. (46).

1. Boundary terms

The boundary product in Eq. (43) ensures that the lattice Boltzmann boundary conditions in Eq. (42) naturally satisfies the boundary terms in Eq. (47). To show this, we consider the first variation of the full-space boundary product,

$$\delta J_{\mathrm{FS}}[\widetilde{\Phi}] = \lim_{\epsilon \to 0^+} \frac{d}{d\epsilon} \Bigg\{ \sum_{\mathrm{sgn}(y) c_{y,i_y} > 0} c_{y,i_y} w_{i_y} \widehat{\widetilde{\Phi}}(y, c_{y,i_y}) \times [\widehat{\widetilde{\Phi}}(y, -c_{y,i_y}) - (1-\alpha)\widehat{\widetilde{\Phi}}(y, c_{y,i_y}) - 2\alpha u_{\partial\Omega}(y)] \Bigg\}_{y=-\frac{1}{2}}^{y=\frac{1}{2}},$$

which can be written as

$$\delta J_{\mathrm{FS}}[\widetilde{\Phi}] = \Bigg\{ \sum_{\mathrm{sgn}(y) c_{y,i_y} > 0} c_{y,i_y} w_{i_y} \sum_{m_y=0}^{M_y} \frac{H_{m_y}(c_{y,i_y})}{m_y!} \sum_{n=0}^{M_y} (a_{1,n}\phi_{1,m_y} + \phi_{1,n} a_{1,m_y}) \frac{1}{n!} \times [H_n(-c_{y,i_y}) - (1-\alpha) H_n(c_{y,i_y})] - 2\alpha u_{\partial\Omega}(y) \phi_{1,m_y} \Bigg\}_{y=-\frac{1}{2}}^{y=\frac{1}{2}}.$$

The terms involving $H_n(c_{y,i_y})$ are symmetric about the exchange of indices, n and m_y, while the terms involving $H_n(-c_{y,i_y})$ are antisymmetric, allowing these summations to be rewritten,

$$\delta J_{\mathrm{FS}}[\widetilde{\Phi}] = \Bigg(\sum_{\mathrm{sgn}(y) c_{y,i_y} > 0} c_{y,i_y} w_{i_y} \sum_{m_y=0}^{M_y} 2 \frac{H_{m_y}(c_{y,i_y})}{m_y!} \phi_{1,m_y} \Bigg\{ \sum_{n=0}^{M_y} \frac{a_{1,n}}{n!} \Bigg[\frac{H_n(-c_{y,i_y})}{2} - (1-\alpha) H_n(c_{y,i_y}) \Bigg] - \alpha u_{\partial\Omega}(y) \Bigg\} + \sum_{m_y=0}^{M_y} \phi_{1,m_y} \sum_{n=0}^{M_y} I_{n,m_y}^{\mathrm{sgn}(y)} a_{1,n} \Bigg)_{y=-\frac{1}{2}}^{y=\frac{1}{2}}, \tag{48}$$

where the summations, $I_{n,m_y}^{\pm}$, are defined by

$$I_{n,m_y}^{\pm} \equiv \frac{1}{n! m_y!} \sum_{c_{y,i_y} \gtrless 0} c_{y,i_y} w_{i_y} H_n(c_{y,i_y}) H_{m_y}(-c_{y,i_y}).$$

We then return to the first boundary term in Eq. (47). Inspection of the definitions of the operator, $\mathbb{L}$, in Eq. (39) and the integral, $\mathcal{L}$, in Eq. (45) shows that only the spatial derivative terms in the definition of $\mathbb{L}$ contribute to the first boundary term in Eq. (47), i.e.,

$$\begin{aligned} \sum_{m_y=0}^{M_y} \left[\phi_{1,m_y} \frac{\partial \mathcal{L}}{\partial\left(\frac{\partial}{\partial y} a_{1,m_y}\right)} \right]_{y=-\frac{1}{2}}^{y=\frac{1}{2}} &= -\sum_{m_y=0}^{M_y} \left[\phi_{1,m_y} \sum_{n=0}^{M_y} \sum_{n'=0}^{M_y} a_{1,n} \mathfrak{I}_{n,n'} \frac{\partial \frac{\partial}{\partial y} a_{1,n'}}{\partial\left(\frac{\partial}{\partial y} a_{1,m_y}\right)} \right]_{y=-\frac{1}{2}}^{y=\frac{1}{2}} \\ &= -\sum_{m_y=0}^{M_y} \left[\phi_{1,m_y} \sum_{n=0}^{M_y} a_{1,n} \mathfrak{I}_{n,m_y} \right]_{y=-\frac{1}{2}}^{y=\frac{1}{2}}, \end{aligned} \tag{49}$$

where

$$\mathfrak{I}_{n,m_y} \equiv \int_{-\infty}^{\infty} c_y w_{1\mathrm{D}}(c_y) \frac{H_n(c_y) H_{m_y}(-c_y)}{n! m_y!} dc_y. \tag{50}$$

This integral is evaluated exactly in this section and the next, in two different ways—with and without the use of Gauss-Hermite quadrature—to facilitate the calculation under consideration.

In this section, it is noted that the integrand in Eq. (50) is a polynomial of order $\leqslant 2M_y + 1$, so Gauss-Hermite quadrature with $M_y + 1$ abscissas and weights evaluate these integrals exactly, i.e.,

$$\mathfrak{I}_{n,m_y} = \sum_{i_y=0}^{M_y} \frac{c_{y,i_y} w_{i_y}}{n! m_y!} H_n(c_{y,i_y}) H_{m_y}(-c_{y,i_y}) = I_{n,m_y}^{+} + I_{n,m_y}^{-}.$$

A change of variables, $c_{y,i_y} \to -c_{y,i_y}$, in the I_{n,m_y}^{-} summation gives

$$\mathfrak{I}_{n,m_y} = I_{n,m_y}^{+} - \sum_{c_{y,i_y} > 0} c_{y,i_y} w_{i_y} \frac{H_{m_y}(c_{y,i_y}) H_n(-c_{y,i_y})}{n! m_y!}, \tag{51}$$

while that same change of variables in the I^{+}_{n,m_y} summation produces

$$\mathfrak{I}_{n,m_y} = I^{-}_{n,m_y} - \sum_{c_{y,i_y}<0} c_{y,i_y} w_{i_y} \frac{H_{m_y}(c_{y,i_y}) H_n(-c_{y,i_y})}{n! m_y!}. \tag{52}$$

Substituting Eqs. (51) and (52) into the first boundary term, Eq. (49), and adding it to the second boundary term, Eq. (48), reduces the expression for the boundary terms to

$$\begin{aligned}
&\sum_{m_y=0}^{M_y} \left[\phi_{1,m_y} \frac{\partial \mathcal{L}}{\partial\left(\frac{\partial}{\partial y} a_{1,m_y}\right)} \right]_{y=-\frac{1}{2}}^{y=\frac{1}{2}} + \delta J_{\mathrm{FS}}[\widetilde{\Phi}] \\
&\quad = \Bigg(\sum_{\mathrm{sgn}(y) c_{y,i_y}>0} c_{y,i_y} w_{i_y} \sum_{m_y=0}^{M_y} 2 \frac{H_{m_y}(c_{y,i_y})}{m_y!} \phi_{1,m_y} \\
&\qquad \times \left\{ \sum_{n=0}^{M_y} \frac{a_{1,n}}{n!} \left[H_n(-c_{y,i_y}) - (1-\alpha) H_n(c_{y,i_y}) \right] \right. \\
&\qquad \left. - \alpha u_{\partial\Omega}(y) \right\} \Bigg)_{y=-\frac{1}{2}}^{y=\frac{1}{2}}.
\end{aligned} \tag{53}$$

The LBM boundary conditions in Eq. (31) zero the summation over n in Eq. (53). This establishes that Eq. (31) are the natural boundary conditions for this variational formulation.

2. Euler-Lagrange equations

Next, we turn our attention to the Euler-Lagrange equations in Eq. (46) so that the (1,)–moments of the Hermite-polynomial expansion of the distribution function, Eq. (41), satisfy the linearized Boltzmann-BGK equation, Eq. (36). Applying the linearized Boltzmann-BGK operator, Eq. (39), to Eq. (41), gives

$$\mathbb{L}\widetilde{\Phi} = \sum_{m_y=0}^{M_y} \frac{c_y H_{m_y}(c_y)}{m_y!} \frac{\partial a_{1,m_y}}{\partial y} + \frac{1}{\mathrm{Kn}} \sum_{m_y=1}^{M_y} \frac{H_{m_y}(c_y)}{m_y!} a_{1,m_y},$$

which becomes

$$\begin{aligned}
\mathbb{L}\widetilde{\Phi} = &\sum_{m_y=0}^{M_y} \frac{H_{m_y+1}(c_y) + m_y H_{m_y-1}(c_y)}{m_y!} \frac{\partial a_{1,m_y}}{\partial y} \\
&+ \frac{1}{\mathrm{Kn}} \sum_{m_y=1}^{M_y} \frac{H_{m_y}(c_y)}{m_y!} a_{1,m_y},
\end{aligned}$$

on application of the recursion relation for Hermite polynomials. The integral of Eq. (45) is easily evaluated from the orthogonality relation and the parity of Hermite polynomials, giving

$$\mathcal{L} = -\sum_{m_y=0}^{M_y} \sum_{n=0}^{M_y} a_{1,n} \frac{\partial a_{1,m_y}}{\partial y} \mathfrak{I}_{n,m_y} + \frac{1}{\mathrm{Kn}} \sum_{m_y=1}^{M_y} \frac{(-1)^{m_y}}{m_y!} a_{1,m_y}^2.$$

In contrast to the previous section, the integrals in Eq. (50) are evaluated exactly without using Gauss-Hermite quadrature,

$$\begin{aligned}
\mathfrak{I}_{n,m_y} &= \frac{(-1)^{m_y}}{n! m_y!} \int_{-\infty}^{\infty} c_y w_{1\mathrm{D}}(c_y) H_n(c_y) H_{m_y}(c_y)\, dc_y \\
&= \frac{(-1)^{m_y}}{n! m_y!} \int_{-\infty}^{\infty} w_{1\mathrm{D}} H_{n+1} H_{m_y}\, dc_y \\
&\quad + \frac{n(-1)^{m_y}}{n! m_y!} \int_{-\infty}^{\infty} w_{1\mathrm{D}} H_{n-1} H_{m_y}\, dc_y \\
&= \frac{(-1)^{n+1}}{n!} (\delta_{n+1,m_y} + n\, \delta_{n-1,m_y}),
\end{aligned} \tag{54}$$

which when substituted into $\mathcal{L}$ produces

$$\begin{aligned}
\mathcal{L} = &\sum_{n=0}^{M_y-1} \frac{(-1)^n}{n!} a_{1,n} \frac{\partial a_{1,n+1}}{\partial y} + \sum_{n=1}^{M_y} \frac{(-1)^n}{(n-1)!} a_{1,n} \frac{\partial a_{1,n-1}}{\partial y} \\
&+ \frac{1}{\mathrm{Kn}} \sum_{n=1}^{M_y} \frac{(-1)^n}{n!} a_{1,n}^2.
\end{aligned} \tag{55}$$

Equation (55) can be written in two further ways that makes the computation of the Euler-Lagrange equations in Eq. (46) clearer:

$$\begin{aligned}
\mathcal{L} = &a_{1,0} \frac{\partial a_{1,1}}{\partial y} + \sum_{n=1}^{M_y-1} \frac{(-1)^n}{n!} a_{1,n} \left(\frac{\partial a_{1,n+1}}{\partial y} + n \frac{\partial a_{1,n-1}}{\partial y} \right) \\
&+ \sum_{n=1}^{M_y} \frac{(-1)^n}{\mathrm{Kn}\, n!} a_{1,n}^2 + \frac{(-1)^{M_y}}{(M_y-1)!} a_{1,M_y} \frac{\partial a_{1,M_y-1}}{\partial y},
\end{aligned} \tag{56a}$$

$$\begin{aligned}
\mathcal{L} = &-a_{1,1} \frac{\partial a_{1,0}}{\partial y} + \sum_{n=1}^{M_y-1} \frac{(-1)^{n+1}}{n!} \left(n\, a_{1,n-1} + a_{1,n} \frac{\partial a_{1,n-1}}{\partial y} \right) \\
&+ \sum_{n=1}^{M_y} \frac{(-1)^n}{\mathrm{Kn}\, n!} a_{1,n}^2 + \frac{(-1)^{M_y+1}}{(M_y-1)!} a_{1,M_y-1} \frac{\partial a_{1,M_y}}{\partial y}.
\end{aligned} \tag{56b}$$

Substituting Eqs. (56a) and (56b) into the first and second terms of Eq. (46), respectively, yields the M_y+1 coupled linear (1,)–moment equations in Eq. (30); their associated boundary conditions follow from Eq. (53) and are identical to Eq. (31). That is, the variational approach gives the final result of the moment method reported in Sec. III. This is achieved without any reference to the original system of $(M_x+1)(M_y+1)$ nonlinear coupled PDEs generated by the moment method (that require sophisticated mathematical manipulations). As such, the variational approach presents a strong improvement in computational efficiency.

V. APPLICATION TO STEADY COUETTE FLOW USING THE D2Q9 LATTICE

This section reports exact analytical solutions for steady Couette flow with arbitrary accomodation at the solid walls, according to the *D2Q9* lattice Boltzmann model. This makes use of Eqs. (30) and (31), which are most efficiently derived using the proposed variational method, as discussed above. A full derivation of the bulk velocity, shear stress and distribution function is presented in Appendix A. Calculations for the *D2Q16* lattice are also given in Sec. S7 of the Supplemental

Material [30]. These analytical solutions can be used in future to benchmark lattice Boltzmann simulations with arbitrary accommodation at the solid walls.

Solving Eqs. (30) and (31), on the $D2Q9$ lattice, gives the following expressions for the bulk velocity and shear stress:

$$u = a_{1,0}(y) = \frac{(u_2 - u_1)y}{1 + 2\sqrt{3}\left(\frac{2}{\alpha} - 1\right)\mathrm{Kn}} + \frac{u_2 + u_1}{2}, \quad (57a)$$

$$P_{xy} = a_{1,1}(y) = \frac{\mathrm{Kn}(u_1 - u_2)}{1 + 2\sqrt{3}\left(\frac{2}{\alpha} - 1\right)\mathrm{Kn}}. \quad (57b)$$

Note that the density has been scaled to unity, and thus the expression in Eq. (57a) coincides with that for the mass flux.

The corresponding velocity slip coefficient, σ, is defined by the small Knudsen number expansion of the bulk velocity at the bottom wall,

$$u\left(-\frac{1}{2}\right) = u_1 + \sigma\mathrm{Kn}\frac{\partial u^{(0)}}{\partial y}\bigg|_{y=-\frac{1}{2}} + o(\mathrm{Kn}),$$

where

$$u = u^{(0)} + u^{(1)}\mathrm{Kn} + o(\mathrm{Kn}).$$

This gives the following result for the slip coefficient on the $D2Q9$ lattice:

$$\sigma = \sqrt{3}\left(\frac{2}{\alpha} - 1\right).$$

The remaining moments are reported in the Appendix A. Together, they enable the reduced distribution function on the $D2Q9$ lattice to now be calculated.

Components of the $D2Q9$ reduced distribution function are defined by $\widetilde{f}_{i_x,i_y}(y) = \widetilde{f}(y, c_{x,i_x}, c_{y,i_y})$, where $(c_{x,1}, c_{x,2}, c_{x,3}) = (c_{y,1}, c_{y,2}, c_{y,3}) = (-\sqrt{3}, 0, \sqrt{3})$. The reduced distribution function can then be expressed by the vector,

$$\widetilde{\boldsymbol{f}} = [\widetilde{f}_{1,1}, \widetilde{f}_{1,2}, \widetilde{f}_{1,3}, \widetilde{f}_{2,1}, \widetilde{f}_{2,2}, \widetilde{f}_{2,3}, \widetilde{f}_{3,1}, \widetilde{f}_{3,2}, \widetilde{f}_{3,3}]^T, \quad (58)$$

where the superscript T denotes the transpose. Substituting the above-calculated moments into Eq. (58) gives

$$\begin{aligned}\widetilde{\boldsymbol{f}} \approx \frac{1}{3}\Bigg[&\frac{\boldsymbol{V}_0}{12} + \frac{P_{xy}}{4}\left(\boldsymbol{V}_{P_{xy}} + \frac{y}{\mathrm{Kn}\sqrt{3}}\boldsymbol{V}_{yP_{xy}}\right)\\ &+ P_{xy}^2\left(\frac{\boldsymbol{V}_{P_{xy}^2}}{2} + \frac{y}{\sqrt{3}\mathrm{Kn}}\boldsymbol{V}_{yP_{xy}^2} + \frac{y^2}{3\mathrm{Kn}^2}\boldsymbol{V}_{y^2P_{xy}^2}\right)\\ &+ \frac{\mathfrak{a}}{4\sqrt{3}}\boldsymbol{V}_{\mathfrak{a}} + \frac{d_1}{2\sqrt{3}}\boldsymbol{V}_{d_1}\\ &+ \mathfrak{a}P_{xy}\left(\frac{\boldsymbol{V}_{\mathfrak{a}P_{xy}}}{\sqrt{3}} + \frac{y}{3\mathrm{Kn}}\boldsymbol{V}_{y\mathfrak{a}P_{xy}}\right) + \frac{\mathfrak{a}^2}{3}\boldsymbol{V}_{\mathfrak{a}^2}\Bigg],\end{aligned}$$

where

$$\begin{aligned}\boldsymbol{V}_0 &= [1, 4, 1, 4, 16, 4, 1, 4, 1]^T,\\ \boldsymbol{V}_{P_{xy}} &= [1, 0, -1, 0, 0, 0, -1, 0, 1]^T,\\ \boldsymbol{V}_{yP_{xy}} &= [1, 4, 1, 0, 0, 0, -1, -4, -1]^T,\\ \boldsymbol{V}_{\mathfrak{a}} &= [-1, -4, -1, 0, 0, 0, 1, 4, 1]^T,\\ \boldsymbol{V}_{d_1} &= \Bigg[-\frac{1}{2}\exp\left(\frac{y}{\mathrm{Kn}\sqrt{3}}\right), 0, -\frac{1}{2}\exp\left(-\frac{y}{\mathrm{Kn}\sqrt{3}}\right),\\ &\quad \exp\left(\frac{y}{\mathrm{Kn}\sqrt{3}}\right), 0, \exp\left(-\frac{y}{\mathrm{Kn}\sqrt{3}}\right),\\ &\quad -\frac{1}{2}\exp\left(\frac{y}{\mathrm{Kn}\sqrt{3}}\right), 0, -\frac{1}{2}\exp\left(-\frac{y}{\mathrm{Kn}\sqrt{3}}\right)\Bigg]^T,\\ \boldsymbol{V}_{P_{xy}^2} &= [1, 0, 1, -2, 0, -2, 1, 0, 1]^T,\\ \boldsymbol{V}_{yP_{xy}^2} &= \left[\frac{1}{2}, 0, -\frac{1}{2}, -1, 0, 1, \frac{1}{2}, 0, -\frac{1}{2}\right]^T,\\ \boldsymbol{V}_{y^2P_{xy}^2} &= \left[\frac{1}{4}, 1, \frac{1}{4}, -\frac{1}{2}, -2, -\frac{1}{2}, \frac{1}{4}, 1, \frac{1}{4}\right]^T,\\ \boldsymbol{V}_{\mathfrak{a}P_{xy}} &= \left[-\frac{1}{2}, 0, \frac{1}{2}, 1, 0, -1, -\frac{1}{2}, 0, \frac{1}{2}\right]^T,\\ \boldsymbol{V}_{y\mathfrak{a}P_{xy}} &= \left[-\frac{1}{2}, -2, -\frac{1}{2}, 1, 4, 1, -\frac{1}{2}, -2, -\frac{1}{2}\right]^T,\\ \boldsymbol{V}_{\mathfrak{a}^2} &= \left[\frac{1}{4}, 1, \frac{1}{4}, -\frac{1}{2}, -2, -\frac{1}{2}, \frac{1}{4}, 1, \frac{1}{4}\right]^T,\end{aligned}$$

and the above-listed constants are

$$\begin{aligned}\mathfrak{a} &= \frac{u_1 + u_2}{2},\\ d_1 &= \frac{\alpha\mathrm{Kn}^2\sqrt{3}\exp\left(\frac{1}{2\mathrm{Kn}\sqrt{3}}\right)[\alpha(\alpha+4) - 4](u_2 - u_1)^2}{\left(\alpha + \exp\left(\frac{1}{\mathrm{Kn}\sqrt{3}}\right) - 1\right)[\alpha - 2\sqrt{3}(\alpha - 2)\mathrm{Kn}]^2}.\end{aligned}$$

Pure specular reflection from the walls, i.e., $\alpha = 0$, does not allow for momentum transfer to the gas. Thus, solutions to the Boltzmann equation are unspecified when $\alpha = 0$. The solutions reported in this study hold for all values of $\alpha \in (0, 1]$, including the limit $\alpha \to 0^+$ (which differs from $\alpha = 0$, as discussed).

The derived analytical LBM solutions for the bulk velocity and shear stress, using the $D2Q9$ and $D2Q16$ lattices (Supplemental Material [30] section S7), are compared to benchmark direct numerical solutions of the linearized Boltzmann-BGK equation [35,36] in Appendix B.

Mathematica code for the moments and reduced distribution function, on both the $D2Q9$ and $D2Q16$ lattices, are given in the Supplemental Material [30].

VI. SUMMARY

The LBM is a numerical method for obtaining approximate yet accurate solutions to kinetic theory. This study makes a number of contributions to the LBM for steady Couette flow:

(1) The complete moment equations in Eq. (29) were derived for a lattice of arbitrary quadrature order and are nonlinear in general.

(2) The specific subset of moments equations from Eq. (29) with $m_x = 1$ pertain solely to the (1,)–moments, e.g., the bulk velocity (mass flux) and shear stress. This subset of $M_y + 1$ coupled moment equations are purely linear and not an approximation of Eq. (29); see Sec. III.

(3) A Hermite-polynomial-based variational approach to the linearized Boltzmann-BGK equation was formulated that directly produces these $M_y + 1$ coupled linear PDEs discussed in point 2 and their boundary conditions; see Sec. IV B.

(4) Solution for the bulk velocity (mass flux) and shear stress using Eq. (29) requires the sophisticated manipulation of $(M_x + 1)(M_y + 1)$ PDEs; this complication is overcome through use of the variational method in point 3; see Secs. III and IV B.

(5) The above points establish that the variational approach presents a substantial improvement in computational efficiency relative to use of the moment method in Eq. (29). Namely, the number of PDEs in the former approach grows linearly with quadrature order, whereas the latter grows quadratically.

(6) Exact analytical solutions to the two-dimensional isothermal lattice Boltzmann model for steady Couette flow under Maxwell-type boundary conditions were reported; see Sec. V.

(7) Exact analytical solutions for the bulk velocity and shear stress using the $D2Q9$ and $D2Q16$ lattice Boltzmann models were compared to benchmark numerical data for the linearized Boltzmann-BGK equation; see Appendix B.

The proposed variational approach can be used in future to derive exact analytical solutions for alternate LBM quadrature schemes and other flow geometries.

ACKNOWLEDGMENTS

This research is supported by an Australian Government Research Training Program (RTP) Scholarship. Y.S. acknowledges support from Ningbo Natural Science Foundation (Project ID 2022J175).

APPENDIX A: EXACT ANALYTICAL SOLUTION TO THE $D2Q9$ LATTICE

In this Appendix, we solve the Boltzmann-BGK equation for steady Couette flow under Maxwell-type boundary conditions on the $D2Q9$ lattice. This is achieved by first evaluating the moments present in the Hermite-polynomial expansion of the reduced distribution function, Eq. (27). These evaluated moments for Maxwell-type boundary conditions are then compared to those reported by Ansumali *et al.* [21] for diffuse reflection, $\alpha = 1$. Finally, the relationship between the reduced distribution function and the moments is inverted to derive the reduced distribution function components that determine these moments and corresponding macroscopic variables. These results provide benchmark analytical solutions for the LBM.

1. Moment evaluation

The (0,)–moments on the $D2Q9$ velocity set, calculated in Sec. S5 of the Supplemental Material [30], are

$$\rho \equiv a_{0,0} = 1, \quad v \equiv \frac{a_{0,1}}{a_{0,0}} = 0, \quad P_{yy} \equiv a_{0,2} + a_{0,0} = 1. \tag{A1}$$

The PDEs in Eq. (30) for the (1,)–moments of the $D2Q9$ lattice Boltzmann solution are

$$\frac{\partial a_{1,1}}{\partial y} = 0,$$
$$\frac{\partial a_{1,0}}{\partial y} + \frac{\partial a_{1,2}}{\partial y} = -\frac{a_{1,1}}{\mathrm{Kn}},$$
$$2\frac{\partial a_{1,1}}{\partial y} = -\frac{a_{1,2}}{\mathrm{Kn}},$$

whose general solution is

$$a_{1,0}(y) = -\frac{yP_{xy}}{\mathrm{Kn}} + \mathfrak{a}, \tag{A2a}$$
$$a_{1,1}(y) = P_{xy}, \tag{A2b}$$
$$a_{1,2}(y) = 0, \tag{A2c}$$

where the constants, P_{xy} and $\mathfrak{a}$, are to be determined from the boundary conditions.

The abscissas in the $D2Q9$ velocity set are specified by the roots of the third-order Hermite polynomial,

$$H_3(\xi) = \xi^3 - 3\xi = \xi(\xi - \sqrt{3})(\xi + \sqrt{3}),$$

that is, $\xi \in \{-\sqrt{3}, 0, \sqrt{3}\}$. The y-directed velocities in this velocity set are $c_{y,i_y} \in \{-\sqrt{3}, 0, \sqrt{3}\}$, for which the Hermite polynomials are

$$H_1(\pm\sqrt{3}) = \pm\sqrt{3}, \quad H_2(\pm\sqrt{3}) = 2.$$

Making use of these quantities in the boundary condition, Eq. (31), at $y = -1/2$, gives

$$\alpha u_1 = \alpha a_{1,0}\left(-\tfrac{1}{2}\right) + \sqrt{3}(2-\alpha)a_{1,1}\left(-\tfrac{1}{2}\right) + \alpha a_{1,2}\left(-\tfrac{1}{2}\right), \tag{A3}$$

whereas at $y = 1/2$ we obtain

$$\alpha u_2 = \alpha a_{1,0}\left(\tfrac{1}{2}\right) - \sqrt{3}(2-\alpha)a_{1,1}\left(\tfrac{1}{2}\right) + \alpha a_{1,2}\left(\tfrac{1}{2}\right). \tag{A4}$$

For partially diffuse interactions, i.e., $\alpha \in (0, 1]$, we substitute Eq. (A2) into the boundary conditions Eqs. (A3) and (A4), whose solution is

$$a_{1,1} = \frac{\mathrm{Kn}(u_1 - u_2)}{1 + 2\sqrt{3}\left(\frac{2}{\alpha} - 1\right)\mathrm{Kn}},$$
$$\mathfrak{a} = \frac{u_1 + u_2}{2},$$

giving the corresponding bulk velocity and shear stress:

$$u = a_{1,0}(y) = \frac{(u_2 - u_1)y}{1 + 2\sqrt{3}\left(\frac{2}{\alpha} - 1\right)\mathrm{Kn}} + \frac{u_2 + u_1}{2}, \tag{A5a}$$

$$P_{xy} = a_{1,1}(y) = \frac{\mathrm{Kn}(u_1 - u_2)}{1 + 2\sqrt{3}\left(\frac{2}{\alpha} - 1\right)\mathrm{Kn}}. \tag{A5b}$$

The energy flux in the $\hat{\boldsymbol{x}}$ direction, Q_x, may also be evaluated, using

$$Q_x \equiv a_{3,0} + a_{1,2} + 4a_{1,0}.$$

On the $D2Q9$ velocity set, $H_3(c_{x,i_x}) = H_3(c_{y,i_y}) = 0$, which gives $a_{3,0} = a_{0,3} = 0$, resulting in the energy flux,

$$Q_x = 4a_{1,0} = 4\rho u, \tag{A6}$$

The (2,)–moments, which are required to evaluate the energy flux normal to the walls,

$$Q_y \equiv a_{2,1}, \tag{A7}$$

are specified by substituting the (0,)–moments, Eq. (A1), into the PDEs in Eq. (29) and setting $m_x = 2$. This gives the system of PDEs:

$$\begin{aligned}\frac{\partial a_{2,1}}{\partial y} &= \frac{1}{\mathrm{Kn}}\left(a_{1,0}^2 - a_{2,0}\right),\\ \frac{\partial a_{2,0}}{\partial y} + \frac{\partial a_{2,2}}{\partial y} &= -\frac{1}{\mathrm{Kn}}a_{2,1},\\ 2\frac{\partial a_{2,1}}{\partial y} &= -\frac{1}{\mathrm{Kn}}a_{2,2},\end{aligned}$$

the general solution of which is

$$\begin{aligned}a_{2,0} &= \left(-\frac{P_{xy}y}{\mathrm{Kn}} + \mathfrak{a}\right)^2 - \frac{d_1}{\sqrt{3}}\cosh\left(\frac{y}{\sqrt{3}\mathrm{Kn}}\right)\\ &\quad + 2P_{xy}^2 - \frac{d_2}{\sqrt{3}}\sinh\left(\frac{y}{\sqrt{3}\mathrm{Kn}}\right),\end{aligned} \tag{A8a}$$

$$\begin{aligned}a_{2,1} &= 2P_{xy}\left(-\frac{P_{xy}y}{\mathrm{Kn}} + \mathfrak{a}\right) + d_1\sinh\left(\frac{y}{\sqrt{3}\mathrm{Kn}}\right)\\ &\quad + d_2\cosh\left(\frac{y}{\sqrt{3}\mathrm{Kn}}\right),\end{aligned} \tag{A8b}$$

$$a_{2,2} = 4P_{xy}^2 - \frac{2d_1}{\sqrt{3}}\cosh\left(\frac{y}{\sqrt{3}\mathrm{Kn}}\right) - \frac{2d_2}{\sqrt{3}}\sinh\left(\frac{y}{\sqrt{3}\mathrm{Kn}}\right), \tag{A8c}$$

where the constants, d_1 and d_2, are to be determined.

The boundary conditions in Eq. (31) for the (2,)–moments are now specified. For $y = -1/2$ and $c_{y,i_y} = \sqrt{3}$, we have

$$\alpha u_1^2 = \alpha a_{2,0}\left(-\tfrac{1}{2}\right) + \sqrt{3}(2-\alpha)a_{2,1}\left(-\tfrac{1}{2}\right) + \alpha a_{2,2}\left(-\tfrac{1}{2}\right), \tag{A9}$$

whereas for $y = 1/2$ and $c_{y,i_y} = -\sqrt{3}$,

$$\alpha u_2^2 = \alpha a_{2,0}\left(\tfrac{1}{2}\right) - \sqrt{3}(2-\alpha)a_{2,1}\left(\tfrac{1}{2}\right) + \alpha a_{2,2}\left(\tfrac{1}{2}\right). \tag{A10}$$

Substituting Eq. (A8) into Eqs. (A9) and (A10), then gives

$$\begin{aligned}d_1 &= \frac{\alpha\mathrm{Kn}^2\sqrt{3}\exp\left(\frac{1}{2\mathrm{Kn}\sqrt{3}}\right)[\alpha(\alpha+4)-4](u_2-u_1)^2}{\left(\alpha+\exp\left(\frac{1}{\mathrm{Kn}\sqrt{3}}\right)-1\right)[\alpha-2\sqrt{3}(\alpha-2)\mathrm{Kn}]^2},\\ d_2 &= 0.\end{aligned}$$

The remaining normal stress, P_{xx}, and energy flux are determined from these constants, giving

$$P_{xx} = a_{2,0} + a_{0,0} = u^2 + 2P_{xy}^2 - \frac{d_1}{\sqrt{3}}\cosh\left(\frac{y}{\mathrm{Kn}\sqrt{3}}\right) + 1, \tag{A11a}$$

$$Q_y = a_{2,1} = 2P_{xy}\left(-\frac{P_{xy}y}{\mathrm{Kn}} + \mathfrak{a}\right) + d_1\sinh\left(\frac{y}{\sqrt{3}\mathrm{Kn}}\right). \tag{A11b}$$

2. Comparison to Ansumali *et al.* [21] for diffuse reflection

Ansumali *et al.* [21] reported exact analytical solutions for pure diffuse reflection, i.e., $\alpha = 1$, for both $D2Q9$ and $D2Q16$ velocity sets. The Knudsen number used in Ref. [21], denoted Kn^*, is related to the present Knudsen number by

$$\mathrm{Kn}^* = \mathrm{Kn}\sqrt{3}, \tag{A12}$$

with the mean-free-path definitions being the origin of the difference.

Setting $\alpha = 1$ in Eqs. (A5a) and (A5b), and making use of Eq. (A12), gives

$$\begin{aligned}\rho u = a_{1,0}(y) &= \frac{(u_2-u_1)y}{1+2\mathrm{Kn}^*} + \frac{u_1+u_2}{2},\\ P_{xy} = a_{1,1}(y) &= \frac{\mathrm{Kn}^*(u_1-u_2)}{(1+2\mathrm{Kn}^*)\sqrt{3}},\end{aligned}$$

while Eq. (A11) becomes

$$\begin{aligned}P_{xx} &= \frac{\mathrm{Kn}^{*2}(u_2-u_1)^2}{3(1+2\mathrm{Kn}^*)^2}\left[2 - \exp\left(-\frac{1}{2\mathrm{Kn}^*}\right)\cosh\left(\frac{y}{\mathrm{Kn}^*}\right)\right]\\ &\quad + \rho u^2 + 1,\\ Q_y &= \frac{\mathrm{Kn}^*}{\sqrt{3}(1+2\mathrm{Kn}^*)^2}(u_2-u_1)^2\left[\mathrm{Kn}^*\exp\left(-\frac{1}{2\mathrm{Kn}^*}\right)\right.\\ &\quad \left.\times\sinh\left(\frac{y}{\mathrm{Kn}^*}\right) - 2y\right] + 2\mathfrak{a}P_{xy},\end{aligned}$$

which are identical to the results for $D2Q9$ in Ref. [21], as required. The same is true for the energy flux parallel to the walls, Q_x, in Eq. (A6).

3. Evaluation of the reduced distribution function

The reduced distribution function components are defined by $\widetilde{f}_{i_x,i_y}(y) = \widetilde{f}(y, c_{x,i_x}, c_{y,i_y})$, where $(c_{x,1}, c_{x,2}, c_{x,3}) = (c_{y,1}, c_{y,2}, c_{y,3}) = (-\sqrt{3}, 0, \sqrt{3})$, allowing the quadrature approximated moments,

$$a_{m_x,m_y} \approx \sum_{i_x=1}^{3}\sum_{i_y=1}^{3} H_{m_x}(c_{x,i_x})H_{m_y}(c_{y,i_y})\widetilde{f}_{i_x,i_y}(y),$$

to be represented by the matrix equation,

$$\begin{aligned}\boldsymbol{a} &\approx \mathfrak{C}\cdot\widetilde{\boldsymbol{f}},\\ \boldsymbol{a} &= [a_{0,0}, a_{0,1}, a_{0,2}, a_{1,0}, a_{1,1}, a_{1,2}, a_{2,0}, a_{2,1}, a_{2,2}]^T,\\ \widetilde{\boldsymbol{f}} &= [\widetilde{f}_{1,1}, \widetilde{f}_{1,2}, \widetilde{f}_{1,3}, \widetilde{f}_{2,1}, \widetilde{f}_{2,2}, \widetilde{f}_{2,3}, \widetilde{f}_{3,1}, \widetilde{f}_{3,2}, \widetilde{f}_{3,3}]^T,\end{aligned}$$

where $\mathfrak{C}$ is a matrix composed of Hermite-polynomial entries. Alternately, the velocities and corresponding reduced distribution function components may be enumerated by a single index (instead of two, as is convention for the LBM [37]),

giving

$$[\boldsymbol{c}_0, \boldsymbol{c}_1, \boldsymbol{c}_2, \cdots, \boldsymbol{c}_8]^T = c_s\sqrt{3}[(0,0), (1,0), (0,1), (-1,0), (0,-1), (1,1), (-1,1), (-1,-1), (1,-1)]^T,$$
$$\widetilde{\boldsymbol{f}} = [\widetilde{f}_{1,1}, \widetilde{f}_{1,2}, \widetilde{f}_{1,3}, \widetilde{f}_{2,1}, \widetilde{f}_{2,2}, \widetilde{f}_{2,3}, \widetilde{f}_{3,1}, \widetilde{f}_{3,2}, \widetilde{f}_{3,3}]^T$$
$$= [\widetilde{f}_7, \widetilde{f}_3, \widetilde{f}_6, \widetilde{f}_4, \widetilde{f}_0, \widetilde{f}_2, \widetilde{f}_8, \widetilde{f}_1, \widetilde{f}_5]^T.$$

The matrix, $\mathfrak{C}$, is transformed into a Vandermonde matrix, $\mathcal{C}$, via

$$\mathfrak{C} = \mathfrak{Z} \cdot \mathcal{C},$$

through the following invertible matrix:

$$\mathfrak{Z} = \begin{bmatrix} 1 & 0 & 0 & 0 & 0 & 0 & 0 & 0 & 0 \\ 0 & 1 & 0 & 0 & 0 & 0 & 0 & 0 & 0 \\ -1 & 0 & 1 & 0 & 0 & 0 & 0 & 0 & 0 \\ 0 & 0 & 0 & 1 & 0 & 0 & 0 & 0 & 0 \\ 0 & 0 & 0 & 0 & 1 & 0 & 0 & 0 & 0 \\ 0 & 0 & 0 & -1 & 0 & 1 & 0 & 0 & 0 \\ -1 & 0 & 0 & 0 & 0 & 0 & 1 & 0 & 0 \\ 0 & -1 & 0 & 0 & 0 & 0 & 0 & 1 & 0 \\ 1 & 0 & -1 & 0 & 0 & 0 & -1 & 0 & 1 \end{bmatrix}, \quad \mathfrak{Z}^{-1} = \begin{bmatrix} 1 & 0 & 0 & 0 & 0 & 0 & 0 & 0 & 0 \\ 0 & 1 & 0 & 0 & 0 & 0 & 0 & 0 & 0 \\ 1 & 0 & 1 & 0 & 0 & 0 & 0 & 0 & 0 \\ 0 & 0 & 0 & 1 & 0 & 0 & 0 & 0 & 0 \\ 0 & 0 & 0 & 0 & 1 & 0 & 0 & 0 & 0 \\ 0 & 0 & 0 & 1 & 0 & 1 & 0 & 0 & 0 \\ 1 & 0 & 0 & 0 & 0 & 0 & 1 & 0 & 0 \\ 0 & 1 & 0 & 0 & 0 & 0 & 0 & 1 & 0 \\ 1 & 0 & 1 & 0 & 0 & 0 & 1 & 0 & 1 \end{bmatrix},$$

that transforms the Hermite-polynomial entries in $\mathfrak{C}$ to the monomial entries that comprise the Vandermonde matrix. The Vandermonde matrix is expressible as the Kronecker product of two invertible matrices,

$$\mathcal{C} = \mathcal{C}_x \otimes \mathcal{C}_y,$$

where those matrices are

$$\mathcal{C}_x = \mathcal{C}_y = \begin{bmatrix} 1 & 1 & 1 \\ -\sqrt{3} & 0 & \sqrt{3} \\ 3 & 0 & 3 \end{bmatrix},$$

with the corresponding inverse matrices being

$$\mathcal{C}_x^{-1} = \mathcal{C}_y^{-1} = \begin{bmatrix} 0 & -\frac{1}{2\sqrt{3}} & \frac{1}{6} \\ 1 & 0 & -\frac{1}{3} \\ 0 & \frac{1}{2\sqrt{3}} & \frac{1}{6} \end{bmatrix}.$$

The inverse of the Vandermonde matrix is given by the product,

$$\mathcal{C}^{-1} = \mathcal{C}_x^{-1} \otimes \mathcal{C}_y^{-1}.$$

The reduced distribution function components are then determined by inverting the original matrix equation, to give

$$\widetilde{\boldsymbol{f}} \approx \mathfrak{C}^{-1} \cdot \boldsymbol{a},$$

where

$$\mathfrak{C}^{-1} = \left(\mathcal{C}_x^{-1} \otimes \mathcal{C}_y^{-1}\right) \cdot \mathfrak{Z}^{-1} = \frac{1}{36}\begin{bmatrix} 1 & -\sqrt{3} & 1 & -\sqrt{3} & 3 & -\sqrt{3} & 1 & -\sqrt{3} & 1 \\ 4 & 0 & -2 & -4\sqrt{3} & 0 & 2\sqrt{3} & 4 & 0 & -2 \\ 1 & \sqrt{3} & 1 & -\sqrt{3} & -3 & -\sqrt{3} & 1 & \sqrt{3} & 1 \\ 4 & -4\sqrt{3} & 4 & 0 & 0 & 0 & -2 & 2\sqrt{3} & -2 \\ 16 & 0 & -8 & 0 & 0 & 0 & -8 & 0 & 4 \\ 4 & 4\sqrt{3} & 4 & 0 & 0 & 0 & -2 & -2\sqrt{3} & -2 \\ 1 & -\sqrt{3} & 1 & \sqrt{3} & -3 & \sqrt{3} & 1 & -\sqrt{3} & 1 \\ 4 & 0 & -2 & 4\sqrt{3} & 0 & -2\sqrt{3} & 4 & 0 & -2 \\ 1 & \sqrt{3} & 1 & \sqrt{3} & 3 & \sqrt{3} & 1 & \sqrt{3} & 1 \end{bmatrix}.$$

Substituting the moments, $\boldsymbol{a}$, into this equation gives the reduced distribution function components,

$$\widetilde{\boldsymbol{f}} \approx \frac{1}{3}\Bigg[\frac{\boldsymbol{V}_0}{12} + \frac{P_{xy}}{4}\left(\boldsymbol{V}_{P_{xy}} + \frac{y}{\mathrm{Kn}\sqrt{3}}\boldsymbol{V}_{yP_{xy}}\right) + P_{xy}^2\left(\frac{\boldsymbol{V}_{P_{xy}^2}}{2} + \frac{y}{\sqrt{3}\mathrm{Kn}}\boldsymbol{V}_{yP_{xy}^2} + \frac{y^2}{3\mathrm{Kn}^2}\boldsymbol{V}_{y^2P_{xy}^2}\right)$$
$$+ \frac{\mathfrak{a}}{4\sqrt{3}}\boldsymbol{V}_{\mathfrak{a}} + \frac{d_1}{2\sqrt{3}}\boldsymbol{V}_{d_1} + \mathfrak{a}P_{xy}\left(\frac{\boldsymbol{V}_{\mathfrak{a}P_{xy}}}{\sqrt{3}} + \frac{y}{3\mathrm{Kn}}\boldsymbol{V}_{y\mathfrak{a}P_{xy}}\right) + \frac{\mathfrak{a}^2}{3}\boldsymbol{V}_{\mathfrak{a}^2}\Bigg],$$

where

$$\boldsymbol{V}_0 = [1,4,1,4,16,4,1,4,1]^T, \quad \boldsymbol{V}_{P_{xy}} = [1,0,-1,0,0,0,-1,0,1]^T,$$
$$\boldsymbol{V}_{yP_{xy}} = [1,4,1,0,0,0,-1,-4,-1]^T, \quad \boldsymbol{V}_{\mathfrak{a}} = [-1,-4,-1,0,0,0,1,4,1]^T,$$
$$\boldsymbol{V}_{d_1} = \left[-\frac{1}{2}\exp\left(\frac{y}{\mathrm{Kn}\sqrt{3}}\right), 0, -\frac{1}{2}\exp\left(-\frac{y}{\mathrm{Kn}\sqrt{3}}\right), \exp\left(\frac{y}{\mathrm{Kn}\sqrt{3}}\right), 0, \exp\left(-\frac{y}{\mathrm{Kn}\sqrt{3}}\right),\right.$$
$$\left.-\frac{1}{2}\exp\left(\frac{y}{\mathrm{Kn}\sqrt{3}}\right), 0, -\frac{1}{2}\exp\left(-\frac{y}{\mathrm{Kn}\sqrt{3}}\right)\right]^T,$$
$$\boldsymbol{V}_{P_{xy}^2} = [1,0,1,-2,0,-2,1,0,1]^T, \quad \boldsymbol{V}_{yP_{xy}^2} = \left[\frac{1}{2},0,-\frac{1}{2},-1,0,1,\frac{1}{2},0,-\frac{1}{2}\right]^T,$$
$$\boldsymbol{V}_{y^2P_{xy}^2} = \left[\frac{1}{4},1,\frac{1}{4},-\frac{1}{2},-2,-\frac{1}{2},\frac{1}{4},1,\frac{1}{4}\right]^T, \quad \boldsymbol{V}_{\mathfrak{a}P_{xy}} = \left[-\frac{1}{2},0,\frac{1}{2},1,0,-1,-\frac{1}{2},0,\frac{1}{2}\right]^T,$$
$$\boldsymbol{V}_{y\mathfrak{a}P_{xy}} = \left[-\frac{1}{2},-2,-\frac{1}{2},1,4,1,-\frac{1}{2},-2,-\frac{1}{2}\right]^T, \quad \boldsymbol{V}_{\mathfrak{a}^2} = \left[\frac{1}{4},1,\frac{1}{4},-\frac{1}{2},-2,-\frac{1}{2},\frac{1}{4},1,\frac{1}{4}\right]^T.$$

APPENDIX B: COMPARISON OF THE *D2Q9* AND *D2Q16* SOLUTIONS TO BENCHMARK NUMERICAL DATA

In this Appendix, exact analytical solutions for the $D2Q9$ and $D2Q16$ velocity sets in Sec. V and Sec. S7 of the Supplemental Material [30], respectively, are compared to literature benchmark data. Specifically, numerical results for the bulk velocity at the wall and the shear stress (constant throughout the gas) are reported by Li *et al.* [35,36], across a range of Knudsen numbers and accommodation coefficients. This

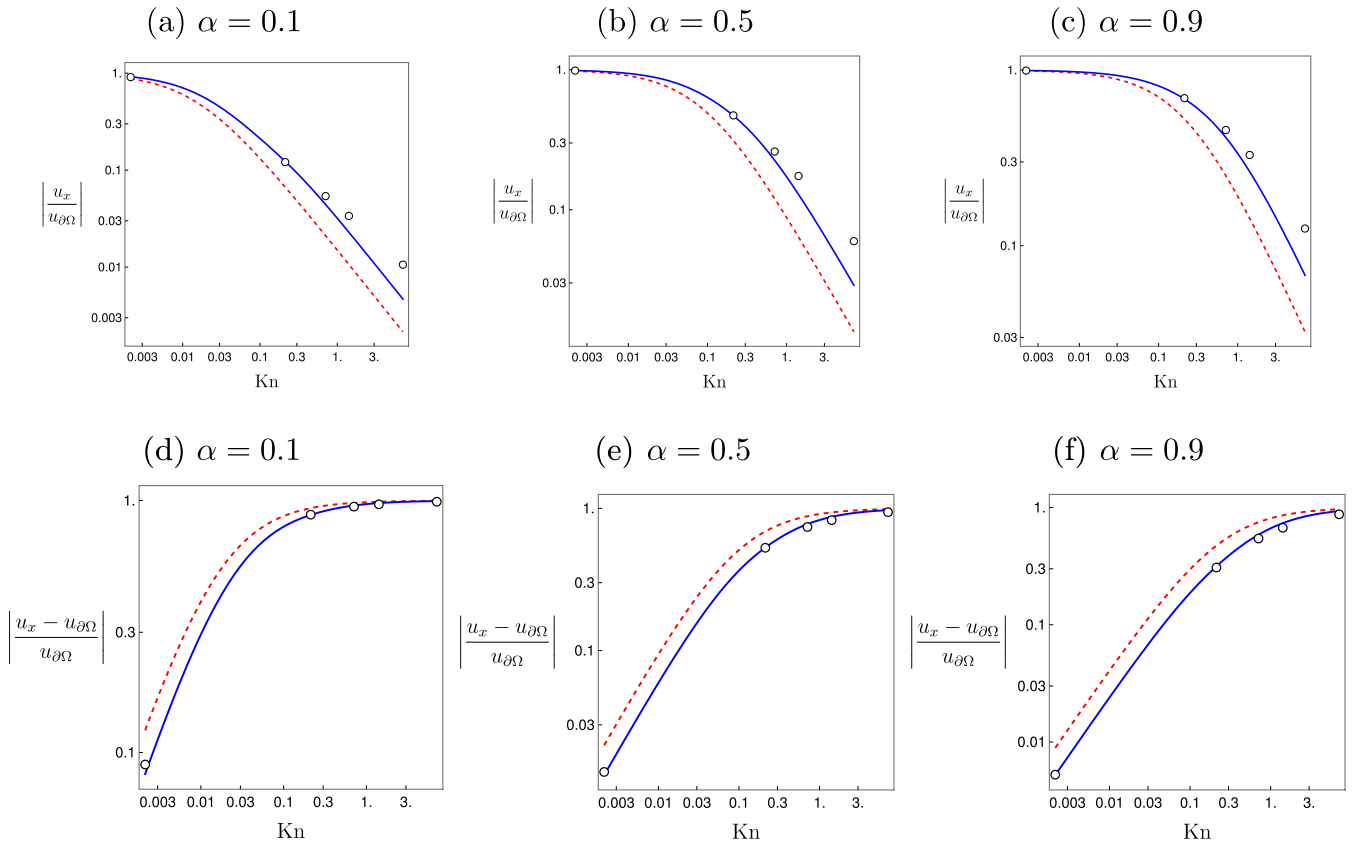

FIG. 2. Scaled bulk wall velocity (top row) and scaled bulk velocity slip at the wall (bottom row) versus Knudsen number, for accommodation coefficients, $\alpha = 0.1, 0.5, 0.9$; wall velocities are $u_{\mathrm{wall}} = \pm 1/2$. Top and bottom rows give the same comparison while highlighting differences for large and small Kn, respectively. Exact analytical solution for $D2Q9$ velocity set [dashed red; Eq. (57a)], exact analytical solution for $D2Q16$ velocity set [solid blue; Eq. (S7.6a) of Supplemental Material [30]], and benchmark data for $\mathrm{Kn} = \frac{3\sqrt{2}}{2000}, \frac{3\sqrt{2}}{20}, \frac{\sqrt{2}}{2}, \sqrt{2}, 5\sqrt{2}$ [circles; Li *et al.* [35,36]].

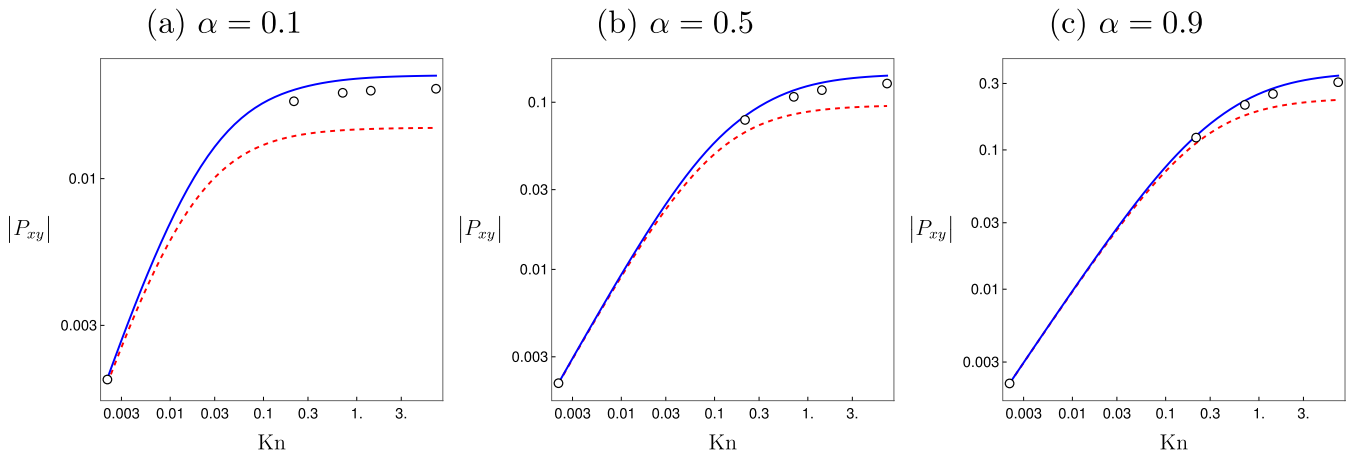

FIG. 3. Dimensionless shear stress versus Knudsen number for accommodation coefficients, $\alpha = 0.1, 0.5, 0.9$; wall velocities are $u_{\text{wall}} = \pm 1/2$. Exact analytical solution for $D2Q9$ velocity set [dashed red; Eq. (57b)], exact analytical solution for $D2Q16$ velocity set [solid blue; Eq. (S7.5b) in the Supplemental Material [30]], and benchmark data for Kn $= \frac{3\sqrt{2}}{2000}, \frac{3\sqrt{2}}{20}, \frac{\sqrt{2}}{2}, \sqrt{2}, 5\sqrt{2}$ [circles; Li *et al.* [35,36]].

literature data is a direct numerical solution of the linearized Boltzmann-BGK equation [38].

Results for the bulk velocity at the wall are given Fig. 2, whereas those for the shear stress are in Fig. 3. As expected, the exact analytical solution for the $D2Q16$ velocity set is more accurate than that for the $D2Q9$ velocity set in all cases, as has been reported previously for purely diffuse reflection [19]. Some differences persist for $D2Q16$ in accord with the use of a finite discrete-velocity set.

[1] G. E. Karniadakis, A. Beskok, and N. Aluru, *Microflows and Nanoflows: Fundamentals and Simulation* (Springer, New York, 2005).

[2] W. Zhang, G. Meng, and X. Wei, A review on slip models for gas microflows, Microfluid. Nanofluid. **13**, 845 (2012).

[3] C. Cercignani, *The Boltzmann Equation and Its Applications* (Springer, New York, 1987).

[4] H. Struchtrup, *Macroscopic Transport Equations for Rarefied Gas Flows: Approximation Methods in Kinetic Theory* (Springer, Berlin, 2006).

[5] Y. Sone, *Molecular Gas Dynamics: Theory, Techniques, and Applications* (Birkhäuser, Boston, MA, 2007).

[6] P. L. Bhatnagar, E. P. Gross, and M. Krook, A model for collision processes in gases 1. Small amplitude processes in charged and neutral one component systems, Phys. Rev. **94**, 511 (1954).

[7] I. Bargatin, I. Kozinsky, and M. L. Roukes, Efficient electrothermal actuation of multiple modes of high-frequency nanoelectromechanical resonators, Appl. Phys. Lett. **90**, 093116 (2007).

[8] H. Grad, On the kinetic theory of rarefied gases, Commun. Pure Appl. Math. **2**, 331 (1949).

[9] H. Grad, Principles of the kinetic theory of gases, in *Thermodynamik der Gase/Thermodynamics of Gases, volume 12 of Handbuch der Physic/Encyclopedia of Physics*, edited by S. Flügge (Springer, Berlin, Heidelberg, 1958), Chap. 3, pp. 205–294.

[10] X. Shan and X. He, Discretization of the velocity space in the solution of the Boltzmann equation, Phys. Rev. Lett. **80**, 65 (1998).

[11] C. Cercignani, A variational principle for boundary value problems in kinetic theory, J. Stat. Phys. **1**, 297 (1969).

[12] R. Benzi, S. Succi, and M. Vergassola, The lattice Boltzmann equation: Theory and applications, Phys. Rep. **222**, 145 (1992).

[13] S. Chen and G. D. Doolen, Lattice Boltzmann method for fluid flows, Annu. Rev. Fluid Mech. **30**, 329 (1998).

[14] G. A. Bird, Approach to translational equilibrium in a rigid sphere gas, Phys. Fluids **6**, 1518 (1963).

[15] G. A. Bird, *Molecular Gas Dynamics* (Clarendon, Oxford, 1976).

[16] G. A. Bird, *Molecular Gas Dynamics and the Direct Simulation of Gas Flows* (Clarendon Press, Oxford, UK, 1994).

[17] S. H. Kim, H. Pitsch, and I. D. Boyd, Accuracy of higher-order lattice Boltzmann methods for microscale flows with finite Knudsen numbers, J. Comput. Phys. **227**, 8655 (2008).

[18] V. E. Ambruş and V. Sofonea, Lattice Boltzmann models based on half-range Gauss–Hermite quadratures, J. Comput. Phys. **316**, 760 (2016).

[19] Y. Shi, P. L. Brookes, Y. W. Yap, and J. E. Sader, Accuracy of the lattice Boltzmann method for low-speed noncontinuum flows, Phys. Rev. E **83**, 045701(R) (2011).

[20] Y. Shi, Y. W. Yap, and J. E. Sader, Linearized lattice Boltzmann method for micro- and nanoscale flow and heat transfer, Phys. Rev. E **92**, 013307 (2015).

[21] S. Ansumali, I. V. Karlin, S. Arcidiacono, A. Abbas, and N. I. Prasianakis, Hydrodynamics beyond Navier–Stokes: Exact solution to the lattice Boltzmann hierarchy, Phys. Rev. Lett. **98**, 124502 (2007).

[22] W. P. Yudistiawan, S. Ansumali, and I. V. Karlin, Hydrodynamics beyond Navier-Stokes: the slip flow model, Phys. Rev. E **78**, 016705 (2008).

[23] Ansumali's moment method has been extended to incorporate Maxwell-type boundary conditions and half-space quadrature [39].

[24] The variational method can be applied to many linearized collision operators and kinetic boundary conditions, as demonstrated by Cercignani [11], but this work will be focused on its application to the linearized-BGK collision model with Maxwell-type boundary conditions.

[25] C. Cercignani, M. Lampis, and S. Lorenzani, Variational approach to gas flows in microchannels, Phys. Fluids **16**, 3426 (2004).

[26] C. Cercignani, M. Lampis, and S. Lorenzani, Plane Poiseuille–Couette problem in micro-electro-mechanical systems applications with gas-rarefaction effects, Phys. Fluids **18**, 087102 (2006).

[27] C. Cercignani and S. Lorenzani, Variational derivation of second-order slip coefficients on the basis of the Boltzmann equation for hard-sphere molecules, Phys. Fluids **22**, 062004 (2010).

[28] S. Lorenzani, Higher order slip according to the linearized Boltzmann equation with general boundary conditions, Phil. Trans. R. Soc. A. **369**, 2228 (2011).

[29] D. R. Ladiges and J. E. Sader, Variational method enabling simplified solutions to the linearized Boltzmann equation for oscillatory gas flows, Phys. Rev. Fluids **3**, 053401 (2018).

[30] See Supplemental Material at http://link.aps.org/supplemental/10.1103/PhysRevE.109.055305 for several mathematical details and examples and which includes Refs. [40–42].

[31] First given in the Appendix to J. C. Maxwell, On stresses in rarified gases arising from inequalities of temperature, Philos. Trans. R. Soc. Lond. **170**, 231 (1879). For a modern discussion see Cercignani [3], pp. 30–35 or Sone [5], pp. 8–9.

[32] The application of Maxwell-type boundary conditions in this work involves a full-space expansion of the reduced distribution function, and so it applies solely to full-space velocity sets.

[33] There are two different conventions for defining Hermite polynomials, depending on whether the argument of the exponential in the weight function, $w_{1D}(\xi)$, is $-\xi^2$ or $-\xi^2/2$. We use the latter convention, which corresponds to the polynomials denoted by He_n in Ref. [43].

[34] M. Madadi, J. T. Johnson, Y. Shi, and J. E. Sader (unpublished).

[35] W. Li, Modeling and simulation of molecular couette flows and related flows, Ph.D. thesis, Old Dominion University, 2015.

[36] W. Li, L. S. Luo and J. Shen, Accurate solution and approximations of the linearized BGK equation for steady Couette flow, Comput. Fluids **111**, 18 (2015).

[37] Y. Shi and J. E. Sader, Lattice Boltzmann method for oscillatory Stokes flow with applications to micro-and nanodevices, Phys. Rev. E **81**, 036706 (2010).

[38] Li *et al.* [35,36] use a different accommodation coefficient and particle velocity scale, which are related to the present definitions by

$$c_{y,\mathrm{Li}} = \sqrt{2}c_y, \quad \alpha = 1 - \alpha_{\mathrm{Li}},$$

where the subscript "Li" denotes to the work of Li *et al.* The corresponding moments are related by

$$\hat{u} = u_{\mathrm{Li}}|_{\mathrm{Kn}_{\mathrm{Li}}=\sqrt{2}\mathrm{Kn},\alpha_{\mathrm{Li}}=1-\alpha}, \quad \hat{p}_{xy} = \sqrt{2}p_{xy,\mathrm{Li}}|_{\mathrm{Kn}_{\mathrm{Li}}=\sqrt{2}\mathrm{Kn},\alpha_{\mathrm{Li}}=1-\alpha}.$$

[39] J. T. Johnson, M. Madadi, B. D. Hughes, D. R. Ladiges, Y. Shi, and J. E. Sader (unpublished).

[40] X. Shan, X. F. Yuan and H. Chen, Kinetic theory representation of hydrodynamics: A way beyond the Navier–Stokes equation, J. Fluid Mech. **550**, 413 (2006).

[41] G. P. Ghiroldi and L. Gibelli, A finite-difference lattice Boltzmann approach for gas microflows, Commun. Comput. Phys. **17**, 1007 (2015).

[42] S. H. Kim and H. Pitsch, Analytic solution for a higher-order lattice Boltzmann method: Slip velocity and Knudsen layer, Phys. Rev. E **78**, 016702 (2008).

[43] M. Abramowitz and I. A. Stegun, *Handbook of Mathematical Functions* (Dover, New York, 1965).